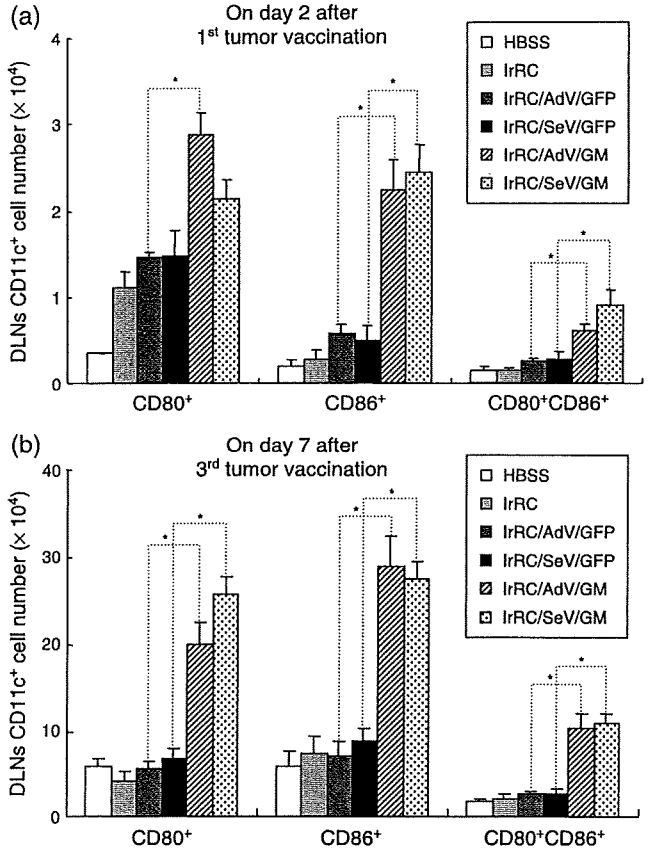


**Fig. 5.** Enhanced recruitment of activated dendritic cells (DC) in draining lymph nodes (DLN) induced with Sendai virus (SeV)- or adenovirus (AdV)-mediated GM-CSF-transduced RENCA vaccine cells. The two left axillary DLN were harvested on (a) day 2 after the first tumor vaccination and (b) day 7 after the third tumor vaccination. The total numbers of $CD11c^+$ cells (DC) expressing costimulatory markers ($CD80^+$, $CD86^+$, $CD80^+$ $CD86^+$) in DLN of mice treated with the indicated tumor vaccination are shown. Bar graphs depict the means ± SEM. Significant differences are denoted with asterisks (*$P < 0.05$). Representative data from two independent experiments are shown.

tumor-antigen specific, as the numbers of IFN-γ- or IL-4-producing cells in the presence of an irrelevant antigen (irradiated WEHI-3B cells) were as low as those in the absence of antigen (Fig. 7b).

We next quantified various inflammatory cytokines produced by splenocytes from mice either left untreated (HBSS only) or treated with irRC/AdV/GFP, irRC/SeV/GFP, irRC/AdV/GM, or irRC/SeV/GM cells. After a 20-h coculture with or without irradiated RENCA cells, supernatants were collected, and the following cytokines were measured: IL-2, IL-4, IL-5, IL-6, IFN-γ, and TNF-α. The IFN-γ, IL-2 (Th1), and IL-4 (Th2) levels produced by splenocytes in the presence of stimulator cells, from mice treated with irRC/AdV/G or irRC/SeV/G cells were significantly higher than those from their respective GFP controls ($P < 0.05$) (Fig. 7d–f). In particular, only the IFN-γ production of restimulated splenocytes from mice treated with irRC/SeV/GM cells was greater than those treated with irRC/AdV/GM cells, which were similar to the results of the ELISPOT assay ($P < 0.05$) (Fig. 7d). Intriguingly, both the IL-2 and IL-6 production levels of restimulated splenocytes from mice treated with irRC/SeV/GFP cells were significantly higher than those treated with irRC/AdV/GFP cells ($P < 0.05$) (Fig. 7e,h). Although the TNF-α and IL-6 production levels of restimulated splenocytes from all mice treated (except for the HBSS-treated group) were markedly elevated, there was no significant difference between those seen in each GFP-treated group and GM-CSF-treated group (Fig. 7c,h). The IL-5 production levels of restimulated splenocytes from mice treated with irRC/AdV/GM or irRC/SeV/GM cells were higher than those treated with their respective GFP controls (irRC/SeV/GM vs irRC/SeV/GFP; $P < 0.05$) (Fig. 7g).

**Characterization of tumor-infiltrating leukocytes induced by irradiated granulocyte macrophage colony-stimulating factor-transduced RENCA vaccine cells.** The tumor microenvironment is composed of an elaborate mixture of tumor- and host-derived cells. To identify the key immune cells that induced the antitumor effects by irradiated GM-CSF-transduced RENCA vaccine cells, the distribution profiles of TIL in RENCA-bearing mice either untreated or treated with the indicated vaccination (irRC/AdV/GFP, irRC/SeV/GFP, irRC/AdV/GM, or irRC/SeV/GM) were assessed by immunohistochemistry. The results showed more infiltrating $CD8^+$ T cells in tumors of mice treated with irRC/AdV/GM or irRC/SeV/GM cells than those treated with their respective controls (irRC/AdV/GFP and irRC/SeV/GFP) ($P < 0.05$). In addition, more infiltrating $CD4^+$ T cells were observed in tumors of mice treated with irRC/SeV/GM cells than in those treated with irRC/SeV/GFP cells ($P < 0.05$) (Fig. 8a). CD11c (DC) and FoxP3 (regulatory T cells) staining was not significantly different among each tumor vaccination group.

To confirm whether the tumor-infiltrating effector cells, $CD8^+$ T cells (CTL), and NK ($DX\text{-}1^+$) cells were in functionally cytolytic conditions, we next quantified comparatively the cell number density of CD107a-expressing $CD8^+$ T and NK cells in tumors during therapeutic tumor vaccination. As shown in Figure 8b, tumor vaccination with irRC/AdV/GM or irRC/SeV/GM cells induced significantly enhanced recruitment of both $CD107a^+CD8^+$ T cells and $CD107a^+$ NK cells into local tumors compared with those induced by their respective controls (irRC/AdV/GFP and irRC/SeV/GFP) ($P < 0.05$).

## Discussion

In the present study, we demonstrated that non-transmissible SeV-mediated GM-CSF-transduced RENCA tumor vaccine cells were effective and well tolerated in mouse therapeutic tumor models, indicating that this novel SeV is a promising gene-delivery vector for clinical GM-CSF-transduced tumor vaccines. The *in vitro* GM-CSF levels produced from various mouse and human tumor cell lines transduced with SeV/dF/mGM or SeV/dF/hGM were equivalent to those transduced with the corresponding adenoviral vectors, which are known to efficiently deliver GM-CSF transgenes (*in vitro* adenovirus transduction; data not shown). Interestingly, although the *in vitro* GM-CSF level produced by irRC/SeV/G cells (643.98 ± 57.61 ng/$10^6$ cells/48 h) was approximately half the amount of that produced by irRC/AdV/GM cells (AdV/G 1250 ± 15.9 ng/$10^6$ cells/48 h), irRC/SeV/GM cells exerted an equivalent antitumor effect compared to that of irRC/AdV/GM cells, and resulted in longer survival than that of irRC/AdV/GM cells in the RENCA-bearing mouse model. Our finding that SeV transduction itself did not have inhibitory effects on the proliferation or viability of RENCA cells *in vitro* could further support the *in vivo* antitumor effect.

The key role of GM-CSF as an immunomodulator is its ability to recruit and activate functional APC[4] such as DC.[2,3,6] In the present study, vaccination with irradiated SeV- or adenovirus-mediated GM-CSF-transduced RENCA cells enhanced the expression of the costimulatory markers CD80 and CD86 on DC in DLN, which elicited lymphadenopathy with marked expansion of these activated DC numbers, whereas differences in the numbers observed between irRC/AdV/GM and irRC/SeV/GM cells were mild. Besides, the total cell numbers of NK ($DX\text{-}5^+$), $CD3^+CD4^+$ T, and $CD3^+CD8^+$ T cells in DLN were also increased when treated with these GM-CSF-transduced RENCA vaccine cells (data not shown). Hence, the ability of overexpressed endogenous GM-CSF to recruit



doi: 10.1111/j.1349-7006.2008.00964.x
© 2008 Japanese Cancer Association

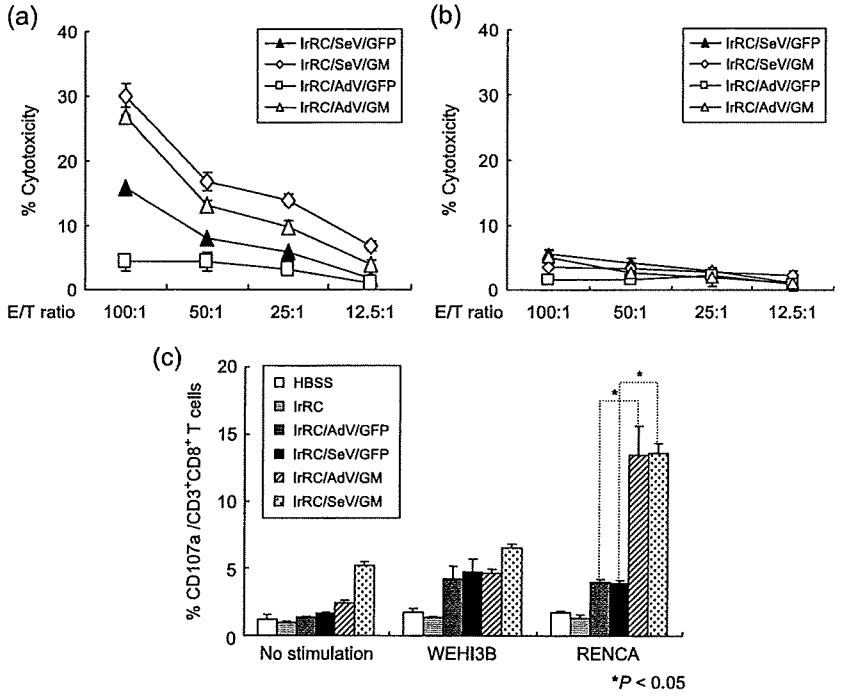


**Fig. 6.** *In vitro* cytotoxicity assays and the effector cells contributing to the antitumor effects induced by the irradiated Sendai virus (SeV)- or adenovirus (AdV)-mediated granulocyte macrophage colony-stimulating factor (GM-CSF)-transduced RENCA vaccine cells. (a,b) Seven days after the third tumor vaccination with irRC/AdV/GFP, irRC/SeV/GFP, irRC/AdV/GM, or irRC/SeV/GM cells, mice were killed to harvest splenocytes. Splenocytes were restimulated with mitomycin C-treated RENCA cells for 6 days and used as effector cells in a $^{51}$Cr-release assay. (a) $^{51}$Cr-labeled RENCA cells used as target cells and (b) WEHI-3B cells used as non-specific target cells were cocultured with effector cells at the indicated effector to target (E : T) ratios for 5 h. (c) CD107a mobilization of splenic CD8$^+$ T cells from mice treated with the indicated tumor vaccinations. Splenocytes were restimulated *in vitro* for 72 h with RENCA cells. The cells were then cultured with or without RENCA or WEHI-3B cells for an additional 5–6 h. The percentages of CD107a-expressing CD3$^+$CD8$^+$ T cells are indicated. The values represent the means ± SEM of the percentage cytotoxicity. Representative data from three independent experiments are shown.

massive numbers of mature DC with enhanced tumor antigen presentation and immunostimulatory functions[1,6,30] as well as other lymphocytes into DLN presumably, in a coordinated manner, activated succeeding effector cells, partially because these relative increases in both CD80 and CD86 expression on DC may lessen the amount of antigen required to trigger T-cell proliferation.[31]

Our results from the *in vitro* cytotoxicity assay, ELISPOT, and enzyme-linked immunosorbent assay using splenocytes showed that the tumor-specific antitumor immunity of the GM-CSF-based immunotherapy was induced through cytolytic CTL and systemic greater production of immunostimulatory cytokines, including IL-2, IFN-γ (Th1 cytokines),[32,33] IL-4,[33,34] IL-5,[32,34] IL-6 (Th2 cytokines),[35] and TNF-α. These findings, taken together with studies assessing the efficacy of GM-CSF-based tumor vaccines in cytokine-deficient mice,[36] suggest principal roles for both Th1 and Th2 immune responses in provoking the antitumor effects of GM-CSF. Among the cytokines measured, elevated IL-5 production induced by GM-CSF-based tumor vaccines suggests that GM-CSF systemically activates eosinophils, which are considered to be involved in GM-CSF-induced antitumor responses.[9,11,34,37]

Our immunohistochemical analysis showed a significant increase in infiltrating CD4$^+$ and CD8$^+$ T cells in tumors treated with irRC/SeV/GM or irRC/AdV/GM cells compared to those treated with their respective GFP controls, consistent with the previous findings that underscored the significance of the number of tumor-infiltrating CD4$^+$ or CD8$^+$ T lymphocytes in antitumor immunity.[36,38,39] In particular, Dranoff *et al.* reported that CD4$^+$ and CD8$^+$ T cells are required for optimal antitumor efficacy elicited by GM-CSF-producing tumor vaccines.[1,3,40] The achievement of immunotherapeutic strategies against cancer depends on the generation of tumor-specific T cells, which can efficiently enter the tumor tissues and interact with target tumor cells mainly by their releasing perforin and granzyme B.[26,27,41,42] Indeed, significantly increased numbers of CD107a-expressing CD8$^+$ T and NK cells were observed in tumors of mice vaccinated with irRC/AdV/GM or irRC/SeV/GM cells (Fig. 8b). In conjunction with our results from the cytotoxicity assay, these results indicate that the GM-CSF-based tumor vaccines promoted to generate both of the functional CTL (adaptive immunity) and NK cells (innate immunity), and these cells are considered to interact to induce antitumor effects *in vivo*.[9,37,40,43]

Whereas remarkable differences between SeV-mediated gene transduction and adenovirus-mediated gene transduction were not observed in our immunological assays, significantly higher IL-6 production by restimulated splenocytes was observed when they were treated with the vaccination of irRC/SeV/GFP cells compared with irRC/AdV/GFP cells. IL-6 is a multifunctional cytokine that controls various immune responses, including inflammation.[35] Grohmann *et al.* reported that IL-6 plays a critical role in mediating the effects of CD40 ligation in DC and enhancing their immunogenicity.[44] Kurooka *et al.* reported that HVJ-E (Sendai virus-envelope) alone eradicates tumors, and speculated that the mechanisms of the antitumor effect of HVJ-E may include a rescue from regulatory T cell-mediated immunosuppression, through dominant IL-6 secretion from DC stimulated with F glycoprotein of HVJ-E.[45,46] Accordingly, our finding that upregulated IL-6 production by splenocytes (including DC) when treated with SeV/dF-based vectors may be one of the advantages of SeV/dF-based vectors over adenovirus-based vectors and may provide us with an encouraging rationale to use them for cancer immune gene therapy. Another expected advantage of the use of SeV/dF-based vectors is that SeV/dF is considered to be safe as it can mediate gene transfer to a cytoplasmic location, evading possible malignant transformation due to nuclear mutations of host cells.[18] Furthermore, actual preclinical achievements in DC-based tumor immunotherapy[22,25] and cancer gene therapy[47,48] using novel SeV vectors have recently been reported.

Despite these beneficial characteristics of SeV, the use of SeV vectors as well as adenovirus vectors has been limited by elevated immune responses to their viral components when administered *in vivo*. However, in the present study, the method of *ex vivo* SeV/dF transduction into autologous tumor cells followed by the removal of nonabsorbed virus could avoid or minimize the intensive immune responses to SeV/dF *in vivo*. Before translating the SeV/dF-mediated autologous GM-CSF-transduced vaccine into a clinical setting, we need to confirm the *ex vivo* transduction efficiencies and the GM-CSF levels produced by primary specimens resected from several cancer patients. Our study showed


© 2008 Japanese Cancer Association

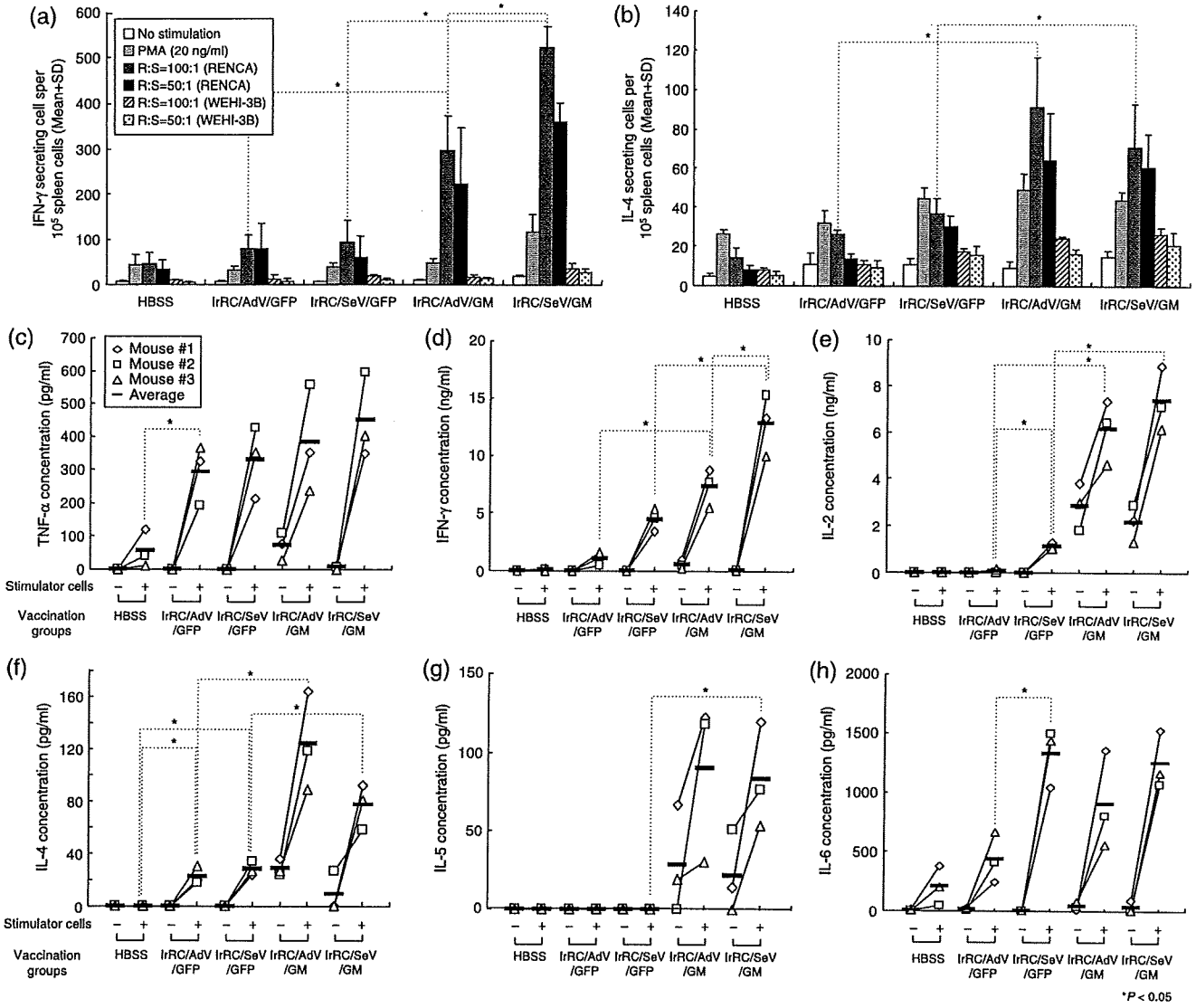


**Fig. 7.** *In vitro* inflammatory cytokine production profiles of splenocytes from mice treated with granulocyte macrophage colony-stimulating factor (GM-CSF)-transduced RENCA vaccine cells. (a,b) Interferon (IFN)-γ and interleukin (IL)-4 production by splenocytes from mice immunized with irRC/AdV/GM or irRC/SeV/GM cells were evaluated using mouse (a) IFN-γ and (b) IL-4 ELISPOT assays. Ten thousand splenocytes, as responder cells (R), from RENCA-bearing mice treated with the indicated tumor vaccines were incubated for 20 h with or without stimulator cells (S) or PMA at the indicated R : S ratios. Bound cytokines were visualized by incubation with biotinylated anti-IFN-γ and anti-IL-4 monoclonal antibodies, followed by streptavidin–horseradish peroxidase, and the premixed peroxidase substrate 3-amino-9-ethylcarbazole (AEC). Results are expressed as the mean number of spot-forming cells + SD from quadruplicate determinations per $1 \times 10^5$ splenocytes. (c–h) Splenocytes were harvested from mice 5 days after the last inoculation of the indicated tumor vaccines and then cocultured with or without irradiated RENCA stimulator cells. Twenty hours after the mixed lymphocyte and tumor incubation, the concentrations of mouse (c) tumor necrosis factor (TNF)-α, (d) IFN-γ, (e) IL-2, (f) IL-4, (g) IL-5, and (h) IL-6 in the culture supernatants were measured by (c–g) cytometric bead array and (h) enzyme-linked immunosorbent assays. $^*P < 0.05$ represents significant difference compared with indicated group.

that irradiated A549 (human lung cancer) cells produced significantly higher levels of GM-CSF *in vitro* than did non-irradiated A549 cells (Fig. 4b). It could be explained by the report that irradiation enhanced the transcription of various genes, including p53 and nuclear factor-κB,[49] as well as their transfection and transduction efficiencies and transgene integration.[50–52] The different effects of irradiation between RENCA and A549 cells are inferred to be dependent on the type or species of tumor cells. In some cases, irradiation may be useful to produce GM-CSF-transduced tumor vaccines from patients' tumors.[53]

In conclusion, we have demonstrated that non-transmissible SeV-mediated GM-CSF-transduced tumor vaccines have antitumor effects on RENCA-bearing mice. Consequently, our results imply, for the first time, that non-transmissible SeV/dF/G could emerge as an alternative, safe vector for cytoplasmic GM-CSF-gene-transduced tumor immunotherapy, although further preclinical investigations using various tumor-cell types are needed.

## Acknowledgments

We thank Mrs Michiyo Okada for excellent technical assistance. We thank Mrs Moboru Kohno, Eisaku Suzuki, Akihiro Tagawa, Takumi Kanaya, Ms Natsuko Kurosawa, and Dr Takashi Hironaka for the preparation and production of SeV vectors. This work was supported by grants from the Ministry of Health, Labour, and Welfare and the Ministry of Education, Culture, Sports, Science and Technology, and Japan Society for the Promotion of Science, Japan.



doi: 10.1111/j.1349-7006.2008.00964.x
© 2008 Japanese Cancer Association

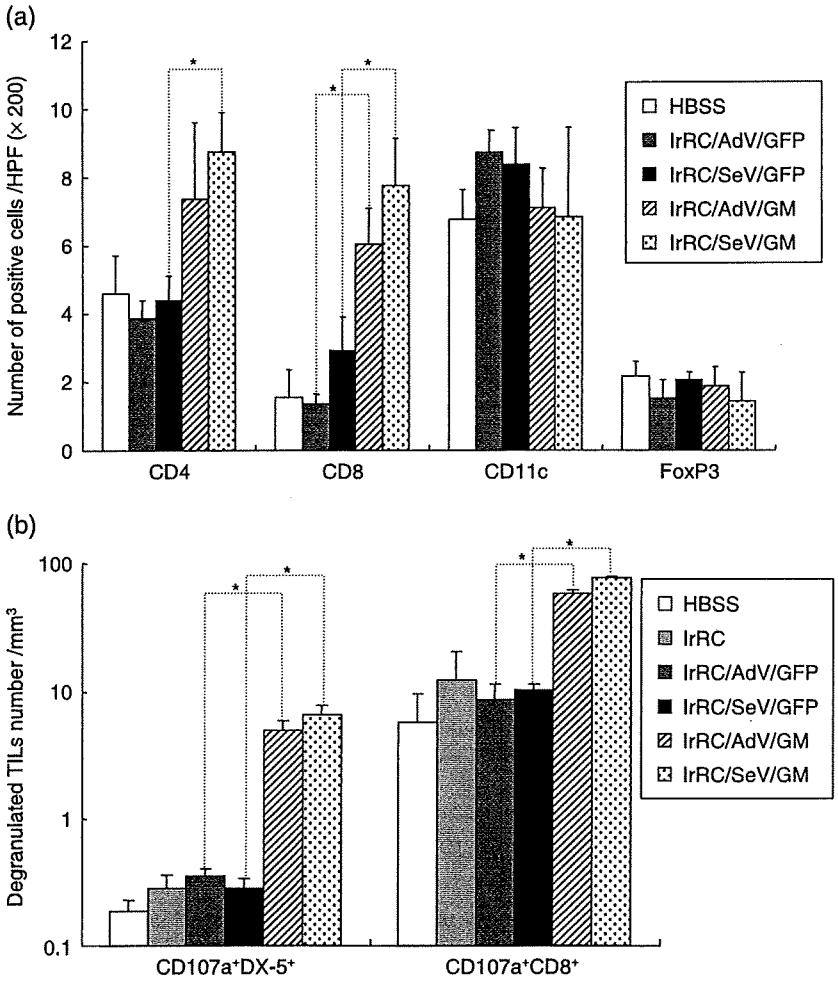


**Fig. 8.** Immunophenotypic analyses of tumor-infiltrating leukocytes by immunohistochemistry and flow cytometry. (a) RENCA-bearing mice were either left untreated (HBSS) or treated with indicated tumor vaccine cells (irRC/AdV/GFP, irRC/SeV/GFP, irRC/AdV/G, and irRC/SeV/G). Resected RENCA tumors were then subjected to immunohistochemical evaluation. To evaluate the distribution of $CD4^+$ T, $CD8^+$ T, $CD11c^+$, and $FoxP3^+$ cells in tumors, positively stained cells were enumerated microscopically at ×200 magnification in 30–70 high-power fields. (b) Enriched viable lymphocytes from mice treated with the tumor vaccination indicated were stained with anti-CD8, anti-DX-5, and antimouse CD107a antibodies and then subjected to flow cytometry. The cell density (divided by the indicated tumor volume [$mm^3$]) of natural killer cells or $CD8^+$ T cells coexpressing degranulated marker of CD107a ($CD107a^+NK^+$ or $CD107a^+CD8^+$ T cells) in tumor-infiltrating leukocytes is shown. Bar graphs depict the means ± SEM. Significant differences are denoted with asterisks ($^*P < 0.05$).

## References


1 Dranoff G, Jaffee E, Lazenby A *et al.* Vaccination with irradiated tumor cells engineered to secrete murine granulocyte-macrophage colony-stimulating factor stimulates potent, specific, and long-lasting anti-tumor immunity. *Proc Natl Acad Sci USA* 1993; **90**: 3539–43.

2 Mach N, Dranoff G. Cytokine-secreting tumor cell vaccines. *Curr Opin Immunol* 2000; **12**: 571–5.

3 Dranoff G. GM-CSF-based cancer vaccines. *Immunol Rev* 2002; **188**: 147–54.

4 Tazi A, Bouchonnet F, Grandsaigne M, Boumsell L, Hance AJ, Soler P. Evidence that granulocyte macrophage-colony-stimulating factor regulates the distribution and differentiated state of dendritic cells/Langerhans cells in human lung and lung cancers. *The J Clin Invest* 1993; **91**: 566–76.

5 Inaba K, Inaba M, Romani N *et al.* Generation of large numbers of dendritic cells from mouse bone marrow cultures supplemented with granulocyte/macrophage colony-stimulating factor. *J Exp Med* 1992; **176**: 1693–702.

6 Miller G, Pillarisetty VG, Shah AB, Lahrs S, Xing Z, DeMatteo RP. Endogenous granulocyte-macrophage colony-stimulating factor overexpression: *in vivo* results in the long-term recruitment of a distinct dendritic cell population with enhanced immunostimulatory function. *J Immunol* 2002; **169**: 2875–85.

7 Steinman RM, Witmer-Pack M, Inaba K. Dendritic cells: antigen presentation, accessory function and clinical relevance. *Adv Exp Med Biol* 1993; **329**: 1–9.

8 Ellem KA, O'Rourke MG, Johnson GR *et al.* A case report: immune responses and clinical course of the first human use of granulocyte/macrophage-colony-stimulating-factor-transduced autologous melanoma cells for immunotherapy. *Cancer Immunol Immunother* 1997; **44**: 10–20.

9 Soiffer R, Lynch T, Mihm M *et al.* Vaccination with irradiated autologous melanoma cells engineered to secrete human granulocyte-macrophage colony-stimulating factor generates potent antitumor immunity in patients with metastatic melanoma. *Proc Natl Acad Sci USA* 1998; **95**: 13 141–6.

10 Simons JW, Jaffee EM, Weber CE *et al.* Bioactivity of autologous irradiated renal cell carcinoma vaccines generated by *ex vivo* granulocyte-macrophage colony-stimulating factor gene transfer. *Cancer Res* 1997; **57**: 1537–46.

11 Tani K, Azuma M, Nakazaki Y *et al.* Phase I study of autologous tumor vaccines transduced with the GM-CSF gene in four patients with stage IV renal cell cancer in Japan: clinical and immunological findings. *Mol Ther* 2004; **10**: 799–816.

12 Simons JW, Mikhak B, Chang JF *et al.* Induction of immunity to prostate cancer antigens: results of a clinical trial of vaccination with irradiated autologous prostate tumor cells engineered to secrete granulocyte-macrophage colony-stimulating factor using *ex vivo* gene transfer. *Cancer Res* 1999; **59**: 5160–8.

13 Jaffee EM, Hruban RH, Biedrzycki B *et al.* Novel allogeneic granulocyte-macrophage colony-stimulating factor-secreting tumor vaccine for pancreatic cancer: a phase I trial of safety and immune activation. *J Clin Oncol* 2001; **19**: 145–56.

14 Salgia R, Lynch T, Skarin A *et al.* Vaccination with irradiated autologous tumor cells engineered to secrete granulocyte-macrophage colony-stimulating factor augments antitumor immunity in some patients with metastatic non-small-cell lung carcinoma. *J Clin Oncol* 2003; **21**: 624–30.

15 Nagai Y. Paramyxovirus replication and pathogenesis. Reverse genetics transforms understanding. *Rev Med Virol* 1999; **9**: 83–99.

16 Markwell MA, Svennerholm L, Paulson JC. Specific gangliosides function as host cell receptors for Sendai virus. *Proc Natl Acad Sci USA* 1981; **78**: 5406–10.

17 Bitzer M, Armeanu S, Lauer UM, Neubert WJ. Sendai virus vectors as an emerging negative-strand RNA viral vector system. *J Gene Med* 2003; **5**: 543–53.




© 2008 Japanese Cancer Association

18 Yonemitsu Y, Kitson C, Ferrari S *et al.* Efficient gene transfer to airway epithelium using recombinant Sendai virus. *Nat Biotechnol* 2000; **18**: 970–3.
19 Moyer SA, Baker SC, Lessard JL. Tubulin: a factor necessary for the synthesis of both Sendai virus and vesicular stomatitis virus RNAs. *Proc Natl Acad Sci USA* 1986; **83**: 5405–9.
20 Kaneda Y, Nakajima T, Nishikawa T *et al.* Hemagglutinating virus of Japan (HVJ) envelope vector as a versatile gene delivery system. *Mol Ther* 2002; **6**: 219–26.
21 Li HO, Zhu YF, Asakawa M *et al.* A cytoplasmic RNA vector derived from nontransmissible Sendai virus with efficient gene transfer and expression. *J Virol* 2000; **74**: 6564–9.
22 Yoneyama Y, Ueda Y, Akutsu Y *et al.* Development of immunostimulatory virotherapy using non-transmissible Sendai virus-activated dendritic cells. *Biochem Biophys Res Commun* 2007; **355**: 129–35.
23 Inoue M, Tokusumi Y, Ban H *et al.* Nontransmissible virus-like particle formation by F-deficient sendai virus is temperature sensitive and reduced by mutations in M and HN proteins. *J Virol* 2003; **77**: 3238–46.
24 Abe J, Wakimoto H, Yoshida Y, Aoyagi M, Hirakawa K, Hamada H. Antitumor effect induced by granulocyte/macrophage-colony-stimulating factor gene-modified tumor vaccination: comparison of adenovirus- and retrovirus-mediated genetic transduction. *J Cancer Res Clin Oncol* 1995; **121**: 587–92.
25 Shibata S, Okano S, Yonemitsu Y *et al.* Induction of efficient antitumor immunity using dendritic cells activated by recombinant Sendai virus and its modulation by exogenous IFN-β gene. *J Immunol* 2006; **177**: 3564–76.
26 Rubio V, Stuge TB, Singh N *et al. Ex vivo* identification, isolation and analysis of tumor-cytolytic T cells. *Nat Med* 2003; **9**: 1377–82.
27 Betts MR, Brenchley JM, Price DA *et al.* Sensitive and viable identification of antigen-specific $CD8^+$ T cells by a flow cytometric assay for degranulation. *J Immunol Meth* 2003; **281**: 65–78.
28 Zhou P, L'Italien L, Hodges D, Schebye XM. Pivotal roles of $CD4^+$ effector T cells in mediating agonistic anti-GITR mAb-induced-immune activation and tumor immunity in CT26 tumors. *J Immunol* 2007; **179**: 7365–75.
29 Vertuani S, De Geer A, Levitsky V, Kogner P, Kiessling R, Levitskaya J. Retinoids act as multistep modulators of the major histocompatibility class I presentation pathway and sensitize neuroblastomas to cytotoxic lymphocytes. *Cancer Res* 2003; **63**: 8006–13.
30 Huang AY, Golumbek P, Ahmadzadeh M, Jaffee E, Pardoll D, Levitsky H. Role of bone marrow-derived cells in presenting MHC class I-restricted tumor antigens. *Science* 1994; **264**: 961–5.
31 Murtaza A, Kuchroo VK, Freeman GJ. Changes in the strength of co-stimulation through the B7/CD28 pathway alter functional T cell responses to altered peptide ligands. *Int Immunol* 1999; **11**: 407–16.
32 Mach N, Gillessen S, Wilson SB, Sheehan C, Mihm M, Dranoff G. Differences in dendritic cells stimulated *in vivo* by tumors engineered to secrete granulocyte-macrophage colony-stimulating factor or Flt3-ligand. *Cancer Res* 2000; **60**: 3239–46.
33 Nakazaki Y, Hase H, Inoue H *et al.* Serial analysis of gene expression in progressing and regressing mouse tumors implicates the involvement of RANTES and TARC in antitumor immune responses. *Mol Ther* 2006; **14**: 599–606.
34 Ellyard JI, Simson L, Parish CR. Th2-mediated anti-tumour immunity: friend or foe? *Tissue Antigens* 2007; **70**: 1–11.
36 Hung K, Hayashi R, Lafond-Walker A, Lowenstein C, Pardoll D, Levitsky H. The central role of $CD4^+$ T cells in the antitumor immune response. *J Exp Med* 1998; **188**: 2357–68.
37 Chu Y, Xia M, Lin Y *et al.* Th2-dominated antitumor immunity induced by DNA immunization with the genes coding for a basal core peptide PDTRP and GM-CSF. *Cancer Gene Ther* 2006; **13**: 510–19.
38 Baskar S, Glimcher L, Nabavi N, Jones RT, Ostrand-Rosenberg S. Major histocompatibility complex class II+B7-$1^+$ tumor cells are potent vaccines for stimulating tumor rejection in tumor-bearing mice. *J Exp Med* 1995; **181**: 619–29.
39 Mumberg D, Monach PA, Wanderling S *et al.* $CD4^+$ T cells eliminate MHC class II-negative cancer cells *in vivo* by indirect effects of IFN-γ. *Proc Natl Acad Sci USA* 1999; **96**: 8633–8.
44 Grohmann U, Fallarino F, Bianchi R *et al.* IL-6 inhibits the tolerogenic function of $CD8\alpha^+$ dendritic cells expressing indoleamine 2,3-dioxygenase. *J Immunol* 2001; **167**: 708–14.
35 Hirano T. Interleukin 6 and its receptor: Ten years later. *Int Rev Immunol* 1998; **16**: 249–84.
40 Dranoff G. GM-CSF-secreting melanoma vaccines. *Oncogene* 2003; **22**: 3188–92.
41 Sadelain M, Riviere I, Brentjens R. Targeting tumours with genetically enhanced T lymphocytes. *Nat Rev* 2003; **3**: 35–45.
42 Gilboa E. The promise of cancer vaccines. *Nat Rev* 2004; **4**: 401–11.
43 Hege KM, Jooss K, Pardoll D. GM-CSF gene-modified cancer cell immunotherapies: of mice and men. *Int Rev Immunol* 2006; **25**: 321–52.
45 Kurooka M, Kaneda Y. Inactivated Sendai virus particles eradicate tumors by inducing immune responses through blocking regulatory T cells. *Cancer Res* 2007; **67**: 227–36.
46 Suzuki H, Kurooka M, Hiroaki Y, Fujiyoshi Y, Kaneda Y. Sendai virus F glycoprotein induces IL-6 production in dendritic cells in a fusion-independent manner. *FEBS Lett* 2008; **582**: 1325–9.
47 Iwadate Y, Inoue M, Saegusa T *et al.* Recombinant Sendai virus vector induces complete remission of established brain tumors through efficient interleukin-2 gene transfer in vaccinated rats. *Clin Cancer Res* 2005; **11**: 3821–7.
48 Kinoh H, Inoue M, Washizawa K *et al.* Generation a recombinant Sendai virus that is selectively activated and lyses human tumor cells expressing matrix metalloproteinases *Gene Ther* 2004; **11**: 1137–45.
49 Vereecque R, Saudemont A, Wickham TJ *et al.* Gamma-irradiation enhances transgene expression in leukemic cells. *Gene Ther* 2003; **10**: 227–33.
50 Stevens CW, Zeng M, Cerniglia GJ. Ionizing radiation greatly improves gene transfer efficiency in mammalian cells. *Human Gene Ther* 1996; **7**: 1727–34.
51 Zeng M, Cerniglia GJ, Eck SL, Stevens CW. High-efficiency stable gene transfer of adenovirus into mammalian cells using ionizing radiation. *Human Gene Ther* 1997; **8**: 1025–32.
52 Teh BS, Aguilar-Cordova E, Vlachaki MT *et al.* Combining radiotherapy with gene therapy (from the bench to the bedside): a novel treatment strategy for prostate cancer. *Oncologist* 2002; **7**: 458–66.
53 Serafini P, Carbley R, Noonan KA, Tan G, Bronte V, Borrello I. High-dose granulocyte-macrophage colony-stimulating factor-producing vaccines impair the immune response through the recruitment of myeloid suppressor cells. *Cancer Res* 2004; **64**: 6337–43.



doi: 10.1111/j.1349-7006.2008.00964.x
© 2008 Japanese Cancer Association

Mol Cell Biochem (2008) 319:181–187
DOI 10.1007/s11010-008-9891-5

# Construction of a high-performance human fetal liver-derived lentiviral cDNA library

**Ryo Kurita · Tatsuo Oikawa · Michiyo Okada · Tomoko Yokoo · Yuusuke Kurihara · Yuko Honda · Rui Kageyama · Youko Suehiro · Toshihiko Okazaki · Mutsunori Iga · Hiroyuki Miyoshi · Kenzaburo Tani**

Received: 27 April 2008 / Accepted: 24 July 2008 / Published online: 15 August 2008
© Springer Science+Business Media, LLC. 2008

**Abstract** The gene transduction method is a very powerful tool, not only in basic science but also in clinical medicine. Regenerative medicine is one field that has close connection with both basic and clinical. Recently, it has been reported that induced pluripotent stem (iPS) cells can be produced from somatic cells by a three or four gene transduction. We have also recently reported that lentiviral gene transfer of the *tal1/scl* gene can efficiently differentiate non-human primate common marmoset ES cells into hematopoietic cells without the support of stromal cells. In this study, we constructed a high-performance human fetal liver-derived lentiviral expression library, which contains a high number of individual clones, in order to develop a very helpful tool for understanding early hematopoiesis and/or hepatocytosis for future regenerative medicine. Our lentiviral cDNA library consisted of more than $8 \times 10^7$ individual clones, and their average insert size was >2 kb. DNA sequence analysis for each individual inserted cDNAs revealed that >60% contained the full-length protein-coding regions for many genes including cytokine receptors, cytoplasmic proteins, protein inhibitors, and nuclear factors. The transduction efficiency on 293T cells was 100% and the average size of an integrated cDNA was ~1.1 kb. These results suggest that our lentiviral human fetal liver cDNA expression library could be a very helpful tool for accelerating the discovery of novel genes that are involved in early hematopoiesis and hepatopoiesis and to make the use of iPS cells more efficient in the field of regenerative medicine.

**Keywords** Lentivirus · Human fetal liver · cDNA expression library · Hematopoiesis · Hepatopoiesis

## Introduction

The gene transduction method is a very powerful tool, both in the field of basic science and in the clinical medicine. In molecular and developmental biology, screening of target genes on various cells, tissues, and organisms have been well studied with various functional analyses [1–4]. Recently, human induced pluripotent stem (iPS) cells have been derived from somatic cells by transduction of three to four genes [5–7], suggesting that the gene transfer method can be a very useful tool for regenerative medicine. Although the development of iPS cells strongly opened the possibility of personalized regenerative medicine, a consolidated method for differentiating iPS has not been established. Recently, we developed a highly efficient method for differentiating hematopoietic cells from non-human primate ES cells, utilizing lentiviral gene transduction, without the addition of stromal cells or growth factors [8]. In murine ES cells, it has been reported that primitive hematopoietic cells, which had some ability to

*Ryo Kurita and Tatsuo Oikawa contributed equally to this work.*

R. Kurita · T. Oikawa · M. Okada · T. Yokoo · Y. Kurihara · Y. Honda · R. Kageyama · Y. Suehiro · T. Okazaki · K. Tani (✉)
Division of Molecular and Clinical Genetics, Department of Molecular Genetics, Medical Institute of Bioregulation, Kyushu University, 3-1-1 Maidashi, Higashi-ku, Fukuoka 812-8582, Japan
e-mail: taniken@bioreg.kyushu-u.ac.jp

M. Iga · K. Tani
Department of Advanced Cell and Molecular Therapy, Kyushu University Hospital, Kyushu University, Fukuoka, Japan

H. Miyoshi
Subteam for Manipulation of Cell Fate, RIKEN BioResource Center, Tsukuba, Ibaraki 305-0074, Japan

reconstitute irradiated-disordered bone marrow, were successfully produced by transduction of the *hoxb4* [9] or *cdx4* [10] genes, suggesting that the transduction of exogenous genes might be a good strategy for the differentiation of specified cells from human iPS and ES cells.

Viral expression libraries have been constructed with gamma retrovirus-based vectors [11–13]. Although these libraries could theoretically introduce genes into mitotic cells, they can also potentially introduce genes in a way that frequently results in leukemia [14]. On the other hand, lentiviral vectors have excellent features for carrying transgenes, including high transduction efficiency leading to an ability to transduce dormant cells, constitutive and long-term expression of transgenes, and the capacity to transduce multiple genes at one time. Kawano et al. constructed a lentiviral library with amplified peripheral leukocyte cDNAs to identify molecules related to cellular resistance to HIV-1 entry and HIV-1-induced cell death [15]. However, a human fetal liver lentiviral cDNA library has not yet been developed.

In this study, we have successfully constructed a high-performance human fetal liver-derived lentiviral expression library, which contained a high number of individual clones, in order to develop a useful research tool for the field of hematopoiesis and/or hepatopoiesis, for future use in clinical regenerative medicine.

## Materials and methods

### Cells

Human 293T cells were maintained in Dulbecco's modified Eagle medium (DMEM) supplemented with 10% heat-inactivated fetal bovine serum (FBS), 100 U/ml penicillin, and 100 mg/ml streptomycin (Nacalai Tesque, Kyoto, Japan), in a humidified atmosphere containing 5% $CO_2$ at 37°C.

### Construction of the lentiviral cDNA library

A CloneMiner cDNA library construction kit (Invitrogen, Carlsbad, CA) was used throughout for preparing the Lentiviral cDNA Library. Double-stranded cDNA was prepared from 5 μg of the human fetal liver poly $(A)^+$ RNA (Clontech, Palo Alto, CA), using Biotin-*att*B2-Oligo (dt) for priming. The blunted cDNA was then ligated to *att*B1 adapters and fractionated using cDNA size fractionation columns (Invitrogen). cDNA fractions (100 ng) >500 bp were incubated with pDONR222 (250 ng) and BP Clonase enzyme mix (Invitrogen) for 18 h at 25°C, and the resulting recombinant sample was electroporated into ElectroMAX DH10B competent cells (Invitrogen). The transformants were pooled, and the resultant entry cDNA library was prepared from pools of transformants using the JETSTAR2.0 plasmid purification kit (Genomed, Lohne, Germany). To generate the lentiviral cDNA vector library, the entry vector (300 ng) and the CSII-CMV-RfA vector (300 ng), which contained *att*R1 and *att*R2 sites, were incubated with LR Clonase enzyme mix (Invitrogen) for 18 h at 25°C. The resulting recombinant molecules were electroporated into ElectroMAX Stbl4 competent cells (Invitrogen), and then the transformants were pooled. To prepare the plasmids for the cDNA library, pools of transformants were plated on LB agar plates containing ampicillin (100 μg/ml), and plasmid purification was carried out from recovered transformants.

### Determining the individual cDNA lengths in the constructed library

The entry cDNA library plasmids and the lentivirus vector cDNA library plasmids were digested with *Bsr*GI (New England Biolabs, Ipswich, MA), subjected to agarose gel electrophoresis, and visualized with ethidium bromide (Sigma, St. Louis, MO). The length of each cDNA was estimated from the sizes of the fluorescent of DNA bands.

### Sequence analysis

cDNAs that were cloned into the CSII-CMV-RfA vector were sequenced with the forward (5′-CAAGCCTCAGACA GTGG-3′) and reverse (5′-AGCGTATCCACATAGCG-3′) primers using a BigDye Terminator v3.1 Cycle sequencing kit (Applied Biosystems, Foster City, CA) and an ABI PRISM 3100 Genetic Analyzer (Applied Biosystems). The sequences were compared with the DNA database from the DNA Data Bank of Japan using BLAST.

### Lentivirus production and transduction with the lentiviral library

Briefly, 34 μg (1–2 × $10^5$ cDNA clones) of the library was mixed with 40 μg of the packaging plasmids (pCAG-HIVg/p and pCMV-VSVG-RSV-Rev) in 3.5 ml of FBS-free DMEM medium, after which 370 μl of 1 mg/ml polyethylenimine (PEI) was added. After incubating for 15–30 min, the DNA/PEI complex was dropped onto semi-confluent 293T cells that were cultured in a T175 flask containing Opti-MEM medium for 3 h. These cells were then cultured in DMEM medium containing 10% FBS. Virus-containing medium was harvested 4 days after the transduction and concentrated by centrifugation (9,000 rpm, 6–8 h, 4°C). The resulting virus pellet was resuspended in 0.5–1 ml of complete DMEM and was used for overnight transduction of freshly prepared 293T cells.

### Determining the individual cDNA lengths in the 293T cells infected lentiviral library

293T cells were transduced with the viral cDNA library and cloned using the limiting dilution method. Genomic DNA was isolated from each clone using the QIAamp DNA Micro Kit (Qiagen). The integrated cDNAs were amplified using PCR, with the forward primer (5′-TTCAGGTGTCGT GAACACGCTACCG-3′) and the reverse primer (5′-CCTC GATGTTAACTCTAGAGGATCC-3′). The Expand Long Template PCR System (Roche, Basel, Switzerland) was used for the PCR. The length of each cDNA was determined as described above.

### Flow cytometry

Untransduced 293T cells and 293T cells that were transduced with the lentivirus library were resuspended at $1 \times 10^6$ cells/100 μl in PBS(−) supplemented with 2% FBS and incubated with FITC-conjugated anti-human glycophorin A (CD235a) antibody (BectonDickinson, Franklin Lakes, NJ). After 30 min at 4°C, the samples were washed twice with PBS/FBS solution and analyzed with a FACS Calibur. Cells were also stained with a FITC-conjugated isotype antibody as negative control. For cell sorting, immunomagnetic beads were used according to the manufacturer's instruction (Miltenyi Biotec, Gladbach, Germany).

## Results

### Construction of the entry cDNA library

To calculate the number of individual clones in the entry library, which was constructed with the gateway system from human fetal liver cDNA, $10^4$, $10^5$, and $10^6$ dilutions of the entry cDNA library transformants (total three lots) were seeded onto LB-Amp plates and incubated overnight at 37°C. As shown in Table 1, the total entry library consisted of $7.87 \times 10^8$ individual clones calculated by counting the number of transformants. We randomly picked 103 colonies, prepared their plasmid DNAs, and digested them with *Bsr*GI. Each plasmid had an insert, and these inserts averaged 2.1 kb in size (Fig. 1a). The cDNA fragments ranged between 0.3 and 6.5 kb in this library, and >40% of the fragments (43.7%) were larger than 2 kb. In particular, about 7.8% of the large insert DNAs, those with fragments lager than 5 kb, were also confirmed. These results indicated that a high titer entry library had successfully been constructed.

### Construction of the lentiviral cDNA library

The lentiviral cDNA library was also prepared using a recombination technique. As shown in Table 2, a library totaling $8.75 \times 10^7$ cfu was constructed. To estimate the average insert size in this library, we picked up 113 colonies and analyzed them as described above. These results showed the library had about a 2.1 kb average insert size (Fig. 1b). This library also contained cDNA fragments that were larger than 5 kb, and more than 40% of the fragments (41.6%) were larger then 2 kb. Sequence analysis of 48 clones demonstrated that >60% (25/40) had genes that encoded various full-length proteins including cytoplasmic enzymes, protein inhibitors, and membrane receptors (the other eight clones had unknown or genomic sequences; Table 3). Furthermore, the presence of typical liver and blood cell markers (such as albumin and hemoglobin) was also confirmed. These data indicated that a high-performance human fetal liver-derived lentiviral cDNA library had successfully been constructed.

**Table 1** Summary of the transformants of the constructed entry cDNA library

| Lot number | Dilution | Amount per plate (μl) | Colonies per plate | Titer (cfu/ml) | Average titer (cfu/ml) | Total volume (ml) | Total CFUs (cfu) |
|---|---|---|---|---|---|---|---|
| 1 | $10^{-4}$ | 100 | 210 | $2.1 \times 10^7$ | $2.37 \times 10^7$ | 12 | $2.84 \times 10^8$ |
| | $10^{-5}$ | 100 | 20 | $2.0 \times 10^7$ | | | |
| | $10^{-6}$ | 100 | 3 | $3.0 \times 10^7$ | | | |
| 2 | $10^{-4}$ | 100 | 202 | $2.02 \times 10^7$ | $2.11 \times 10^7$ | 10 | $2.11 \times 10^8$ |
| | $10^{-5}$ | 100 | 23 | $2.3 \times 10^7$ | | | |
| | $10^{-6}$ | 100 | 2 | $2.0 \times 10^7$ | | | |
| 3 | $10^{-4}$ | 100 | 218 | $2.18 \times 10^7$ | $2.43 \times 10^7$ | 12 | $2.92 \times 10^8$ |
| | $10^{-5}$ | 100 | 21 | $2.1 \times 10^7$ | | | |
| | $10^{-6}$ | 100 | 3 | $3.0 \times 10^7$ | | | |
| | | | | | | | *Final CFU count (cfu)*: $7.87 \times 10^8$ |

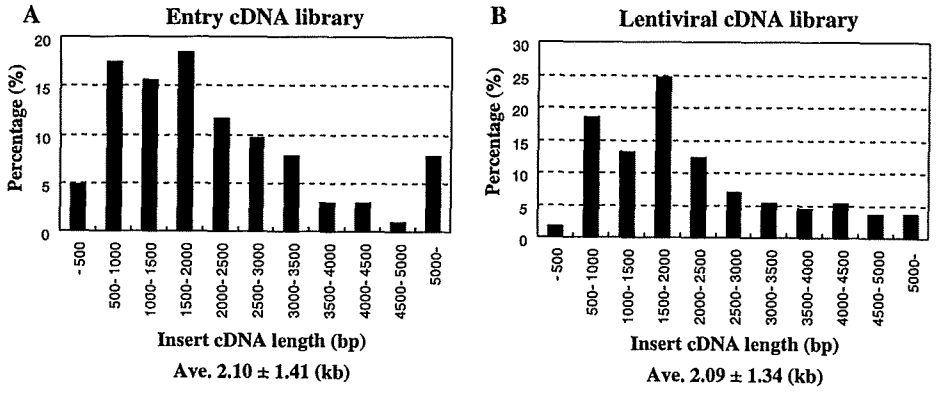


**Fig. 1** The distribution of the cDNA fragments in the constructed entry (a) or lentiviral (b) cDNA libraries. More than 100 *E. coli* colonies in each library were randomly picked and their plasmid DNAs were prepared. Each plasmid was then digested with *Bsr*GI and analyzed. In each library, >40% of the cDNA fragments were >2 kb. Especially, large insert DNAs, namely, fragments >5 kb, were confirmed to be between 3.5% and 7.8% of the total. These data indicate that high titer entry and lentiviral libraries were successfully constructed

**Table 2** Summary of the transformants of the lentiviral cDNA library

| Lot number | Dilution | Amount per plate (μl) | Colonies per plate | Titer (cfu/ml) | Average titer (cfu/ml) | Total volume (ml) | Total CFUs (cfu) |
|---|---|---|---|---|---|---|---|
| 1 | $10^{-3}$ | 100 | 208 | $2.1 \times 10^6$ | $2.16 \times 10^6$ | 10 | $2.16 \times 10^7$ |
| | $10^{-4}$ | 100 | 24 | $2.4 \times 10^6$ | | | |
| | $10^{-5}$ | 100 | 2 | $2.0 \times 10^6$ | | | |
| 2 | $10^{-3}$ | 100 | 397 | $3.97 \times 10^6$ | $3.96 \times 10^6$ | 10 | $3.96 \times 10^7$ |
| | $10^{-4}$ | 100 | 49 | $4.9 \times 10^6$ | | | |
| | $10^{-5}$ | 100 | 3 | $3.0 \times 10^6$ | | | |
| 3 | $10^{-3}$ | 100 | 378 | $3.78 \times 10^6$ | $2.63 \times 10^6$ | 10 | $2.63 \times 10^7$ |
| | $10^{-4}$ | 100 | 21 | $2.1 \times 10^6$ | | | |
| | $10^{-5}$ | 100 | 2 | $2.0 \times 10^6$ | | | |
| | | | | | | | *Final CFU count (cfu)*: $8.75 \times 10^7$ |

## Transduction of the lentivirus libraries into cultured cells

The lentiviral library was produced by transfecting 1–2 × $10^5$ lentiviral cDNAs and an accessory plasmid DNA into freshly prepared 293T cells, after which single cell clones were isolated by limiting dilution. Genomic PCR analysis of 50 clones revealed that the transduction efficiency was 100% and most clones (49/50) had several transgenes (3–10). The average insert size of a transgene was about 1.1 kb and fragments >3 kb were not observed (Fig. 2). Next, to confirm the expression of the transgenes at the protein level, flow cytometric analysis was performed using anti-glycophorinA (GPA) antibody on 293T cells that were transduced with the viral library. GPA is major sialoglycoproteins of the human erythrocyte membrane. In early embryogenesis, hematopoietic, especially erythroid, development is observed in fetal liver, suggesting that various genes related to the development and differentiation of erythroid cells will be abundant in our library. The results showed that the frequency of GPA positive cells was slightly increased in the lentiviral library infected 293T cells compared with the non-transduced cells (0.4% vs. 0.04%, respectively; Fig. 3). This indicated that GPA derived from the library was expressed. To clarify this point more clearly, we sorted GPA positive cells with magnetic beads, cultured them for several days, and analyzed them by flow cytometry. The results showed that the frequency of GPA positive cells isolated from library transduced 293T cells was dramatically increased (up 65.4%), compared to that from the non-transduced cells. These results demonstrated that our lentiviral library could transduce exogenous genes into target cells and furthermore that these genes were expressed in these cells at the protein level.

**Table 3** Sequence analysis of the lentiviral cDNA library

| No. | Inserted length (kb) | Gene | Genbank accession No. | cds size (bp) | Status |
|---|---|---|---|---|---|
| 1 | 2 | Angiotensinogen (AGT) | NM_000029 | 1,458 | F |
| 2 | 2.2 | Interleukin 10 receptor, beta (IL10RB) | NM_000628 | 978 | F |
| 3 | 1.8 | EEF1A1 | NM_001402 | 1,389 | P |
| 4 | 3.3 | Albumin | BC039235 | 1,884 | F |
| 5 | 3.5 | Poliovirus receptor (PVR) | BC015542 | 1,254 | F |
| 6 | 3.6 | SH3-domain GRB2-like endophilin B2 (SH3GLB2) | BC014635 | 1,188 | F |
| 7 | 2.55 | Stearoyl-CoA desaturase (SCD) | AF097514 | 1,080 | P |
| 8 | 0.9 | Ribosomal protein S3A | BC001708 | 795 | F |
| 9 | 1.6 | Heterogeneous nuclear ribonucleoprotein A1 (hnRPA1) | BC071945 | 963 | F |
| 10 | 1.5 | Fibrinogen beta chain | BC107766 | 1,476 | P |
| 11 | 1.3 | Protein inhibitor of activated STAT3 (PIAS3) | AB021868 | 1,860 | P |
| 12 | 0.7 | Hemoglobin, alpha 2 (HBA2) | BC008572 | 429 | F |
| 13 | 1.4 | Aldo-keto reductase family 1, member C1 (AKR1C1) | BC020216 | 972 | F |
| 14 | 2.7 | Damage-specific DNA binding protein 1 (DDB1) | BC011686 | 3,423 | P |
| 15 | 1.3 | Unknown | AC016525 | | |
| 16 | 1.3 | Glyceraldehyde-3-phosphate dehydrogenase (GAPDH) | BC029618 | 1,008 | F |
| 17 | 1.7 | Unknown | AK128092 | | |
| 18 | 0.9 | Ferritin, light polypeptide (FTL) | BC004245 | 528 | F |
| 19 | 1.7 | Insulin-like growth factor II (IGF-2) | X07868 | | P |
| 20 | 0.8 | Heat shock 60 kDa protein 1 (chaperonin) | BC073746 | 1,722 | P |
| 21 | 4.5 | TP53 apoptosis effector variant, PERP | BC010163 | 582 | F |
| 22 | 0.65 | Putative MAPK activating protein | AB097053 | 1,224 | P |
| 23 | 1.4 | Non-specific DNA | | | |
| 24 | 1.9 | Aspatate aminotransferase 1 | BC000498 | 1,242 | F |
| 25 | 7.3 | Aconitase1, soluble (ACO1) | BC018103 | 2,670 | F |
| 26 | 2.8 | Solute carrier family 25, member 46 | BC017169 | 1,257 | F |
| 27 | 1.7 | Ribonuclease P 14 kDa subunit | BC012017 | 375 | F |
| 28 | 1 | Testis enhanced gene transcript (BAX inhibitor 1) | BC000916 | 714 | P |
| 29 | 1.5 | Serpin peptidase inhibitor, clade A, member 1 | BC015642 | 1,257 | F |
| 30 | 3.9 | Histidine acid phosphatase domain containing 1 | BC024591 | | P |
| 31 | 0.65 | Hemoglobin, alpha 2 (HBA2) | BC008572 | 429 | F |
| 32 | 5.7 | Unknown | AF214636 | | |
| 33 | 1.1 | Haptoglobin | BC121125 | 1,221 | P |
| 34 | 1.5 | Cross-immune reaction antigen (VCIA1) | AY858798 | 1,314 | F |
| 35 | 2.2 | Albumin | BC039235 | 1,884 | F |
| 36 | 1.3 | Unknown | AL365360 | | |
| 37 | 0.3 | ATPase, $Na^+/K^+$ transporting, beta 3 polypeptide | BC011835 | 840 | P |
| 38 | 2 | Decorin (DCN) | BC005322 | 1,080 | F |
| 39 | 0.65 | Ribosomal protein L32 pseudogene 3 | BC053996 | | P |
| 40 | 0.6 | Wilm's tumor-related protein (QM) | M64241 | 645 | F |
| 41 | 0.7 | Hemoglobin, beta | BC007075 | 444 | F |
| 42 | 1.3 | Serpin peptidase inhibitor, clade A, member 3 | BC070265 | 288 | F |
| 43 | 1.4 | ras homolog gene family, member B | BC066954 | 591 | P |
| 44 | 1.7 | Genomic DNA | AY495330 | | |
| 45 | 1.7 | Genomic DNA | DQ862537 | | |
| 46 | 3.9 | Genomic DNA | AL024498 | | |
| 47 | 3 | Genomic DNA | AL035461 | | |
| 48 | 0.6 | Hemoglobin, alpha 2 (HBA2) | BC008572 | 429 | F |

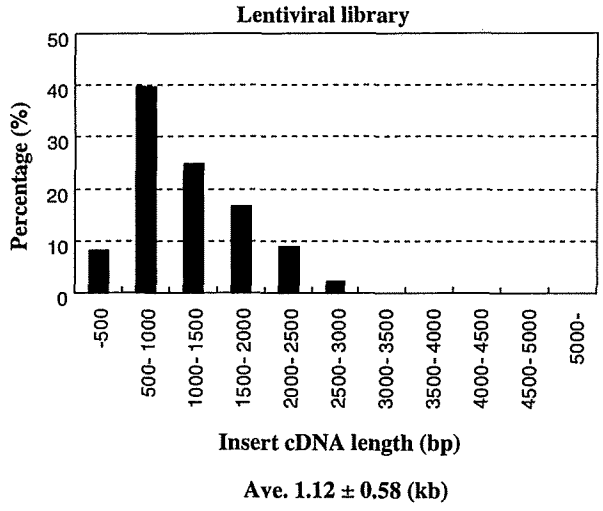


**Fig. 2** The distribution of transgene length in the lentiviral library infected cells. After 293T cells were transfected with 1–2 × $10^5$ lentiviral cDNAs and accessory plasmids, a lentiviral library was produced. Freshly prepared 293T cells were transduced with this virus library, and single cell clones were isolated by limiting dilution. Genomic PCR analysis of 50 clones revealed that the average transgene insert size was ~1.1 kb, and fragments >3 kb were not observed

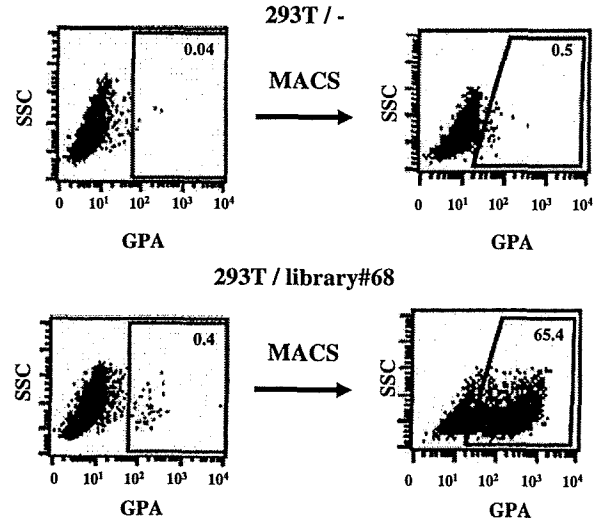


**Fig. 3** Transgenic expression of the lentiviral library by flow cytometry. To confirm the expression of the transgenes at the protein level, virally transduced 293T cells were analyzed using flow cytometry with anti-glycophorinA (GPA). GPA positive cells were slightly increased in the lentiviral library transduced 293T cells (0.4%) compared with the non-transduced cells (0.04%). These GPA positive cells were sorted using magnetic beads, cultured for several days, and analyzed by flow cytometry. These results showed that GPA positive cells, which were isolated from the lentiviral library transduced 293T cells, were dramatically increased (65.4%) compared to non-transduced cells

## Discussion

The library that we constructed in this study had 8.75 × $10^7$ individual clones (100% of which had inserted DNA). The average insert length was about 2.1 kb. Sequence analysis demonstrated that more than 60% of these genes encoded full-length proteins. Moreover, high transduction efficiency was confirmed in cultured cells, and a transduced gene was translated and localized correctly. Kawano et al. successfully constructed a peripheral leukocyte-derived lentiviral cDNA library, which contained 8 × $10^7$ primary clones and an average insert size of 1.26 kb [15]. Our library had almost the same number of insert cDNAs and a larger insert size. Notably, the average size of a gene that was transduced by our virus library was also longer (1.12 vs. 0.71 kb). These results demonstrate that a high-performance human fetal liver-derived lentiviral library was successfully constructed.

Lentiviral vectors can efficiently transduce both dividing and non-dividing cells, including blood and stem cells, which can generally be transduced with a low transduction efficiency [16]. In our experiment, most of the clonal virus-library transduced 293T cells had multiple (>3) transductions, suggesting that the transduction efficiency was high.

In early embryogenesis, most hepatopoietic and hematopoietic development (especially erythroid) is observed in fetal liver, suggesting that various genes related to the development and differentiation of the liver and blood will be abundant in our library. In line with this, some typical hepatocytic and erythroid cell markers (such as albumin and hemoglobin) were identified in our library. Thus, this fetal liver lentivirus library may be a powerful tool for the functional screening and targeting of novel genes that specify hepatocytic and hematopoietic cell development and differentiation.

A method for deriving iPS cells has been recently established [5–7], and therefore, organ regeneration will be a popular treatment for repairing damaged organs. The bone marrow and liver may be good candidates for target organs that require regeneration. Our fetal liver cDNA library may be a very useful tool for determining the genes that are important for differentiating iPS cells into hematopoietic cells or hepatopoietic cells. For example, one could screen ES cells and/or cytokine-dependent cell lines to find novel hematopoietic genes. We previously reported a highly efficient method for differentiating hematopoietic cell from primate ES cells by transducing the *tal1/scl* gene [8]. By combining this system with our fetal liver library, we may be able to direct the production of hematopoietic stem cells from ES cells, which may allow us to substantially impact the field of reproductive medicine in the near future.

## References


1. Wong BY, Chen H, Chung SW et al (1994) High-efficiency identification of genes by functional analysis from a retroviral cDNA expression library. J Virol 68:5523–5531
2. Kassner PD (2008) Discovery of novel targets with high throughput RNA interference screening. Comb Chem High Throughput Screen 11:175–188. doi:10.2174/138620708783877744
3. Caldwell JS (2007) Cancer cell-based genomic and small molecule screens. Adv Cancer Res 96:145–173. doi:10.1016/S0065-230X(06)96006-0
4. Jones AK, Buckingham SD, Sattelle DB (2005) Chemistry-to-gene screens in *Caenorhabditis elegans*. Nat Rev Drug Discov 4:321–330. doi:10.1038/nrd1692
5. Takahashi K, Tanabe K, Ohnuki M et al (2007) Induction of pluripotent stem cells from adult human fibroblasts by defined factors. Cell 131:861–872. doi:10.1016/j.cell.2007.11.019
6. Nakagawa M, Koyanagi M, Tanabe K et al (2008) Generation of induced pluripotent stem cells without Myc from mouse and human fibroblasts. Nat Biotechnol 26:101–106. doi:10.1038/nbt1374
7. Yu J, Vodyanik MA, Smuga-Otto K et al (2007) Induced pluripotent stem cell lines derived from human somatic cells. Science 318:1917–1920. doi:10.1126/science.1151526
8. Kurita R, Sasaki E, Yokoo T et al (2006) Tal1/Scl gene transduction using a lentiviral vector stimulates highly efficient hematopoietic cell differentiation from common marmoset (*Callithrix jacchus*) embryonic stem cells. Stem Cells 24:2014–2022. doi:10.1634/stemcells.2005-0499
9. Kyba M, Perlingeiro RC, Daley GQ (2002) HoxB4 confers definitive lymphoid-myeloid engraftment potential on embryonic stem cell and yolk sac hematopoietic progenitors. Cell 109:29–37. doi:10.1016/S0092-8674(02)00680-3
10. Wang Y, Yates F, Naveiras O et al (2005) Embryonic stem cell-derived hematopoietic stem cells. Proc Natl Acad Sci USA 102:19081–19086. doi:10.1073/pnas.0506127102
11. Rayner JR, Gonda TJ (1994) A simple and efficient procedure for generating stable expression libraries by cDNA cloning in a retroviral vector. Mol Cell Biol 14:880–887
12. Whitehead I, Kirk H, Kay R (1995) Expression cloning of oncogenes by retroviral transfer of cDNA libraries. Mol Cell Biol 15:704–710
13. Kitamura T (1998) New experimental approaches in retrovirus-mediated expression screening. Int J Hematol 67:351–359. doi:10.1016/S0925-5710(98)00025-5
14. Hacein-Bey-Abina S, Von Kalle C, Schmidt M et al (2003) LMO2-associated clonal T cell proliferation in two patients after gene therapy for SCID-X1. Science 302:415–419. doi:10.1126/science.1088547
15. Kawano Y, Yoshida T, Hieda K et al (2004) A lentiviral cDNA library employing lambda recombination used to clone an inhibitor of human immunodeficiency virus type 1-induced cell death. J Virol 78:11352–11359. doi:10.1128/JVI.78.20.11352-11359.2004
16. Bai Y, Soda Y, Izawa K et al (2003) Effective transduction and stable transgene expression in human blood cells by a third-generation lentiviral vector. Gene Ther 10:1446–1457. doi:10.1038/sj.gt.3302026

ELSEVIER

Experimental Hematology

Experimental Hematology 2008;36:1634–1641

# Bioluminescent evaluation of the therapeutic effects of total body irradiation in a murine hematological malignancy model

Yusuke Inoue[a], Kiyoko Izawa[b], Shigeru Kiryu[c], Seiichiro Kobayashi[b], Arinobu Tojo[b], and Kuni Ohtomo[c]

[a]*Department of Radiology, Institute of Medical Science, University of Tokyo, Tokyo, Japan;* [b]*Division of Molecular Therapy, Advanced Clinical Research Center, Institute of Medical Science, University of Tokyo, Tokyo, Japan;* [c]*Department of Radiology, Graduate School of Medicine, University of Tokyo, Tokyo, Japan*

(Received 28 June 2008; revised 18 August 2008; accepted 20 August 2008)

*Objective.* **We investigated the utility of in vivo bioluminescence imaging (BLI) in assessing the therapeutic effects of total body irradiation (TBI) in a murine hematological malignancy model.**

*Materials and Methods.* **The suspension of Ba/F3 cells transduced with firefly luciferase and p190 BCR-ABL genes was exposed to ionizing radiation, and viable cell numbers and bioluminescent signals were measured serially. Mice intravenously inoculated with the cells underwent TBI at various doses. In vivo BLI was performed repeatedly until spontaneous death, and whole-body bioluminescence signals were determined as an indicator of whole-body tumor burden.**

*Results.* **In the cell culture study, bioluminescence signals generally reflected viable cell numbers, despite some overestimation immediately after irradiation. Sublethal TBI in mice transiently depressed the increase in whole-body signals and prolonged survival. Spontaneous death occurred at similar signal levels regardless of radiation dose. A significant negative correlation was found between survival and whole-body signal early after TBI. Significant dose dependence was demonstrated for both survival and signal increase early after TBI and was more evident for signal increase. Lethally irradiated mice without bone marrow transplantation died while showing weak signals. In mice receiving lethal TBI and syngeneic bone marrow transplantation, signal reduction and prolongation of survival were prominent, and whole-body signals at death were similar to those in nonirradiated or sublethally irradiated mice.**

*Conclusion.* **In vivo BLI allows longitudinal, quantitative evaluation of the response to TBI in mice of a hematological malignancy model. Antitumor effects can be assessed early and reliably using in vivo BLI.** © **2008 ISEH - Society for Hematology and Stem Cells. Published by Elsevier Inc.**

In vivo bioluminescence imaging (BLI) allows noninvasive, whole-body evaluation of luciferase expression in intact small animals and is used increasingly to evaluate the effects of novel therapeutic strategies against malignant neoplasms [1,2]. For bioluminescent tumor monitoring, mice are inoculated with tumor model cells stably expressing firefly luciferase. Injection of the mice with D-luciferin, substrate for firefly luciferase, induces light emission from the cells, and images that reflect the amount and distribution of the inoculated cells can be acquired repeatedly in individual animals.

In vivo BLI has been applied to studies using animal models of hematological malignancies [3–8]. In hematological malignancy models, various organs, including bone marrow, lymph nodes, liver, and spleen may be involved and, because of the difficulty in assessing whole-body tumor burden, therapeutic effects are evaluated in conventional experiments primarily based on survival. However, in addition to the time-consuming nature of survival assessment, survival may be affected by various confounding factors other than the antitumor effects of the therapeutic intervention, and many animals are required to yield

Offprint requests to: Yusuke Inoue, MD, Department of Radiology, Institute of Medical Science, University of Tokyo, 4-6-1 Shirokanedai, Minato-ku, Tokyo 108-8639, Japan; E-mail: inoueys-tky@umin.ac.jp

0301-472X/08 $–see front matter. Copyright © 2008 ISEH - Society for Hematology and Stem Cells. Published by Elsevier Inc.
doi: 10.1016/j.exphem.2008.08.004

statistically relevant results. Deaths from tumor progression need to be discriminated from treatment-related or accidental deaths. Because of the limitations of survival assessment, in vivo BLI may be particularly beneficial for animal experiments of hematological malignancies.

It has been validated in various tumor models that the intensity of light signals determined from in vivo BLI reflects tumor burden quantitatively [9–18]. However, most studies have assessed the relationship between tumor size and BLI signal without therapeutic interventions, and validation studies concerning tumors after therapy are limited. Some studies have revealed discrepancies between tumor sizes and BLI signals in treated animals [17–19]. Although these discrepancies were attributed to BLI reflecting viable tumors selectively, whereas tumor size measurements are affected by necrotic or fibrotic components of the tumor and were interpreted as evidence of the superiority of BLI over size measurements, the reliability of BLI assessment of therapeutic efficacy and posttreatment regrowth has not been fully established.

Radiotherapy, including total body irradiation (TBI), plays an important role as a treatment option for hematological malignancies [20], and further improvements of treatment strategies, including optimization of radiation dose, schedule, and field design, use of a radiosensitizer or radioprotector, and combinations with other treatment modalities, are being pursued [21–24]. Animal experiments using in vivo BLI may aid such investigations. In this study, we evaluated in vitro relationships between viable cell number and luminescent intensity longitudinally after exposing luciferase-expressing cells of a hematological malignancy model to ionizing radiation. Moreover, mice inoculated intravenously with the cells underwent TBI at various doses with or without bone marrow transplantation (BMT). In vivo BLI was performed repeatedly until spontaneous death, and the effects of the different treatments were monitored in individual mice based on survival and BLI signals. The principal aim of this study was to determine the potential of in vivo BLI for assessment of the therapeutic efficacy of TBI in mice of a hematological malignancy model.

## Materials and methods

*Cell lines*

The interleukin-3–dependent murine pro–B-cell line Ba/F3 was cotransfected with the firefly luciferase gene and the wild-type p190 BCR-ABL fusion gene using a retroviral method described previously [25]. Stable transfectants were selected, and the established cells were named Ba/F3-Luc/Wt cells. The cDNA encoding firefly luciferase was excised from the pGL3-basic vector (Promega, Madison, WI, USA), and the long terminal repeat (LTR) of Moloney murine leukemia virus (MMLV) drives luciferase expression in the Ba/F3-Luc/Wt cells. A single cell clone isolated by limiting dilution was used in all experiments. The subclone used in this study was different from that used in the previous study [3] and was selected because of its consistent in vivo proliferation. The p190 BCR-ABL gene is important in the development of acute lymphoblastic leukemia [26] and causes factor-independent, autonomous proliferation when transformed into Ba/F3 cells [27]. The Ba/F3-Luc/Wt cells were maintained in RPMI-1640 medium (Invitrogen, Grand Island, NY, USA) supplemented with 10% (v/v) fetal bovine serum (JRH Biosciences, Lenexa, KS, USA) and 1% penicillin/streptomycin (Invitrogen) in the absence of interleukin-3. Cell cultures were incubated at 37°C in 5% $CO_2$.

*Animals*

Eight-week-old female BALB/c nu/nu mice were inoculated with $2 \times 10^6$ Ba/F3-Luc/Wt cells, suspended in 0.1 mL phosphate-buffered saline (PBS), intravenously via the tail vein and were used as a hematological malignancy animal model. Mice were obtained from SLC Japan (Hamamatsu, Japan) and were handled in accordance with guidelines of the Institute of Medical Science, the University of Tokyo. Experiments were approved by the committee for animal research at the institution.

*In vitro analysis*

Viable cell counting, standard luciferase assay, intact-cell luciferase assay, and cell cycle analysis were performed to assess proliferation and bioluminescent features of the cultured cells. All measurements were performed in triplicate. Viable cell numbers and viability were measured using the trypan blue dye exclusion method and hemocytometers.

Luciferase activity in a given volume of cell suspension, containing various numbers of cells, was determined by a standard luciferase assay. After centrifugation of 100 μL cell suspension, the pellet was lysed with 200 μL lysis buffer (Passive Lysis Buffer; Promega). The lysate was centrifuged, and the supernatant was stored at –80°C until assayed. Luciferase activity in the supernatant was measured using the Luciferase Assay Reagent (Promega), according to the manufacturer's recommendation and using a plate reader (Wallac ARVO MX 1420 Multilabel Counter; Perkin Elmer Japan, Yokohama, Japan). Luminescence was also measured by simply adding D-luciferin (Beetle Luciferin Potassium Salt; Promega) to the cell suspension without cell lysis. We refer to this as the intact-cell luciferase assay. Cell suspension (20 μL) was added to D-luciferin (100 μL 180 μg/mL solution), and the light output was measured using the plate reader. Phenol red-free RPMI-1640 medium was used for the cell culture study to avoid possible light absorbance by the dye.

To assess the cell cycle, cells were fixed with cooled 70% ethanol. Afterward, fixed cells were washed twice with PBS and incubated with 0.5% ribonuclease A for 30 minutes. After the addition of propidium iodide (final concentration, 25 μg/mL), cells were analyzed by flow cytometry using a FACSCalibur flow cytometer (Becton Dickinson, Franklin Lakes, NJ, USA). The cell cycle was determined using the FlowJo software (TreeStar, San Carlos, CA, USA). The fraction of proliferating cells, or the proliferation index, was calculated by the following equation:

$$\text{Proliferation index}(\%) = (G_2/M+)/(G_1/G_0 + SG_2/M + S) \times 100,$$

where $G_2/M$, S, and $G_1/G_0$ are the numbers of cells in the $G_2/M$, S, and $G_1/G_0$ phases, respectively.

*Radiation of cell suspension*

To investigate the validity of bioluminescent monitoring of the effect of ionizing radiation, we irradiated the suspension of Ba/F3-Luc/Wt cells in vitro and evaluated the time course of bioluminescent signals in relation to viable cell numbers. In vitro measurements were performed on days 0, 2, 3, 5, 7, 9, and 11. Immediately after day-2 measurements, the cell suspension was irradiated with 5 Gy using a $^{137}Cs$ source (Gammacell 1000 Elite; MDS Nordion, Kanata, Ontario, Canada) at a dose rate of 6.4 Gy/min. The culture medium was changed after each set of measurements, and the cell suspension was diluted so that the culture density remained below $3.5 \times 10^5$ cell/mL. The viable cell number and luminescence in a given volume of cell suspension were corrected for dilution ratios and expressed as a percentage of day-0 values.

*In vivo BLI*

In vivo BLI was performed using a cooled charge coupled device camera system (IVIS Imaging System 100; Xenogen, Alameda, CA, USA). Mice received an intraperitoneal injection of 150 mg/kg D-luciferin and were placed in the light-tight chamber of the camera system under isoflurane anesthesia. Beginning 5 minutes after injection, photographic and luminescent images in the dorsal, left-lateral, ventral, and right-lateral projections were acquired. The data acquisition series of four projections was repeated twice; consequently, a single imaging session provided eight luminescent images. Luminescent images were taken with an exposure time of 1 to 60 seconds, binning of 4 or 8, and a field-of-view of 25 cm. Up to five mice were imaged simultaneously.

*Monitoring after sublethal TBI*

Mice inoculated with Ba/F3-Luc/Wt cells underwent sublethal TBI, and the therapeutic effects were monitored using in vivo BLI longitudinally. In vivo BLI was performed 5 days after cell inoculation, and mice were divided into four groups (n = 5 each), one control group and three TBI groups, which had comparable whole-body signals 5 days postinoculation. Seven days after inoculation, the mice underwent in vivo BLI and were then irradiated with various single radiation doses. TBI was performed using a 150-kV x-ray source (MBR-1520R-3; Hitachi, Tokyo, Japan) operating at 20 mA and filtered with 1 mm Al at a rate of 1.81 Gy/min. The three TBI groups were given doses of 3, 4, or 5 Gy, and the control group was sham irradiated. In vivo BLI was performed 8, 10, and 14 days after cell inoculation (1, 3, and 7 days after TBI) and then twice a week until spontaneous death.

*Monitoring after lethal TBI*

Mice inoculated with Ba/F3-Luc/Wt cells underwent lethal TBI with or without BMT, and were examined by in vivo BLI longitudinally. In vivo BLI was performed before and 5 days after cell inoculation, and mice were divided into two groups (n = 5 each), the TBI alone group and the TBI + BMT group, which had comparable whole-body signals 5 days postinoculation. Seven days after inoculation, the mice underwent in vivo BLI and thereafter TBI of 7 Gy. This dose was shown to be above the LD100/30 in preliminary experiments. The BMT was performed for the TBI + BMT group 24 hours after TBI. Bone marrow cells harvested from the femurs and tibias of syngeneic mice ($2 \times 10^7$ cells in 0.2 mL PBS) were injected via the tail vein. In vivo BLI was performed 10 and 14 days after the inoculation of Ba/F3-Luc/Wt cells (3 and 7 days after TBI) and then twice a week up to 63 days after inoculation. After the day-63 study, only one mouse showing slowly increasing BLI signals remained alive, and BLI was performed once a week until the spontaneous death of the mouse.

*Data analysis*

To assess whole-body tumor burden from in vivo BLI, a region of interest (ROI) encompassing the entire mouse except the tail and distal ends of the limbs was placed on each in vivo BLI image, and the total signal in the ROI (photons/s) was quantified using the Living Image software (version 2.50; Xenogen). The total signals of all eight images obtained in a single imaging session were averaged to determine the whole-body signal, which was used as a marker of whole-body tumor burden. The 14/7-day signal ratio was determined as the ratio of the whole-body signal 14 days after cell inoculation (7 days after TBI) to that 7 days after inoculation (just before TBI). To assess whole-body tumor burden at spontaneous death, the day of spontaneous death was recorded based on a daily check of survival, and presumptive whole-body signal at death was calculated by extrapolating from the final two data points monoexponentially.

In the study of sublethal TBI, comparisons between groups were made by one-way analysis of variance followed by post-hoc analysis using Fisher's least significant difference tests. Survival was compared with the whole-body signal by linear regression analysis. Statistical testing was conducted after logarithmic transformation of bioluminescence signals and signal ratios. A $p$ value $<0.05$ was considered statistically significant.

## Results

*Radiation of cell suspension*

We irradiated Ba/F3-Luc/Wt cells in vitro and evaluated the relationship between cell proliferation and temporal changes in luminescence. Viable cell counting showed depression of cell proliferation 1 day after irradiation and regrowth 7 days after irradiation (Fig. 1A). Viability (Fig. 1C) and proliferation index (Fig. 1D) declined 3 days and 1 day after irradiation, respectively. Both standard and intact-cell luciferase assays demonstrated radiation-induced inhibition of the increase in luminescent signals from a given amount of cell suspension, consistent with depression of cell proliferation (Fig. 1A). However, luminescent signals definitely increased 1 day after irradiation despite minimal augmentation in viable cell number, and correspondingly, luminescence per cell increased (Fig. 1B). The discrepancy between luminescence and viable cell number diminished gradually, and luciferase assays faithfully demonstrated regrowth.

*Monitoring after sublethal TBI*

Mice received sublethal TBI (3, 4, or 5 Gy) 7 days after intravenous inoculation of Ba/F3-Luc/Wt cells, and in vivo BLI was repeated until spontaneous death. Twenty mice,

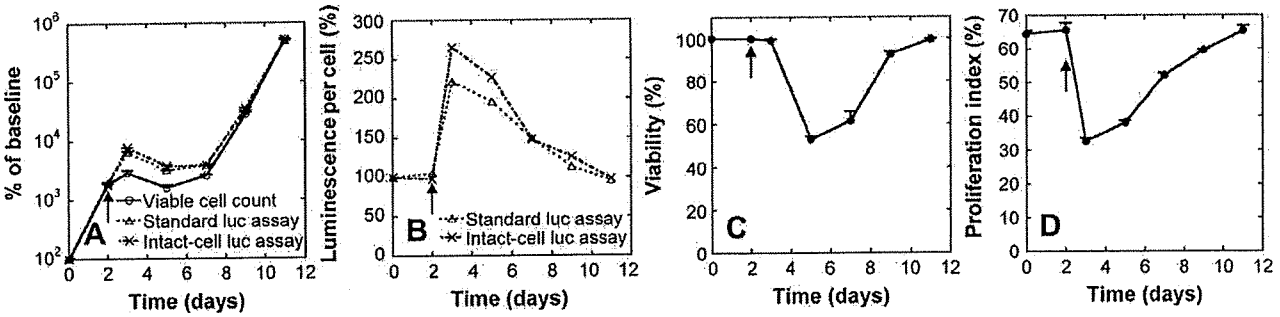


**Figure 1.** Irradiation of cultured Ba/F3-Luc/Wt cells. The viable cell number, and luminescent signals from the standard luciferase assay and the intact-cell luciferase assay, expressed as percentages of baseline values, increased before irradiation, and the increase was inhibited after irradiation performed on day 2 (**A**). The inhibition was delayed for luminescence, and luminescence per cell increased transiently after irradiation (**B**). Viability (**C**) and proliferation index (**D**) decreased early after irradiation. Arrows indicate the day of irradiation, and error bars represent standard deviations (n = 3).

including nonirradiated control mice, were studied 8 to 12 times, and 189 BLI studies in total were performed, regarding a series of image acquisitions as consisting of five BLI studies when five mice were imaged simultaneously. Unexpectedly, essentially no signals were detected in five studies, suggesting bowel injection of D-luciferin [9,28]. In such cases, D-luciferin was injected again, resulting in reasonable luminescence, and the signals obtained after the second injection were used for analysis.

In vivo BLI demonstrated focal luminescent signals indicative of tumor cell proliferation before TBI (Fig. 2). Control mice showed consistent increases in whole-body signals over time and died 27 to 29 days after cell inoculation (Fig. 3). Bone marrow signals appeared to be dominant early after inoculation, and signals in the spleen and liver became conspicuous later. TBI caused transient inhibition of increase in whole-body signals and prolonged survival in a dose-dependent manner. Signals increased 1 day after TBI, similar to the control group, and decreased thereafter. Regrowth tended to be delayed after greater radiation doses. Spontaneous death occurred at similar signal levels, regardless of radiation dose. The presumptive whole-body signal at death had a relatively narrow range, from $6.70 \times 10^9$ to $2.16 \times 10^{10}$ photons/s, for all 20 mice and did not differ significantly among groups.

A significant negative correlation was found between survival and whole-body signals 14 days after inoculation, 7 days after TBI (Fig. 4; $r = -0.8000$, $p < 0.0001$). Survival differed significantly among groups (Fig. 5A; $p < 0.01$) and tended to be longer in mice receiving greater doses although it was marginally shorter in the 4-Gy group than in the 3-Gy group. In the post-hoc analysis, significant differences were demonstrated between controls and the 3-Gy group, between controls and the 5-Gy group, and between the 4-Gy and 5-Gy groups, but not between controls and the 4-Gy group, between the 3-Gy and 4-Gy groups, or between the 3-Gy and 5-Gy groups. The 14/7-d signal ratio, indicating signal increase during 7 days after TBI, differed significantly among groups (Fig. 5B; $p < 0.0001$) and was smaller in mice receiving greater doses. Dose dependence was more evident for the 14/7-d signal ratio than for survival, and the post hoc analysis of the 14/7-d signal ratio vs dose showed significant differences for all pairs.

*Monitoring after lethal TBI*

Mice underwent lethal TBI (7 Gy) with or without BMT and were followed by repeated in vivo BLI. In total, 118 BLI studies were performed and additional D-luciferin injection was required in four studies because of apparent injection failure.

Lethal TBI caused profound reduction in whole-body signals (Fig. 6), although residual disease was demonstrated even at maximal reduction by both visual evaluation and quantitative analysis of the BLI images. Mice in the TBI alone group died 20 to 22 days after cell inoculation while whole-body signals remained weak, consistent with treatment-related death. In the TBI + BMT group, in vivo BLI showed minimal signals 17 days after inoculation (10 days after TBI), followed by regrowth. The 14/7-d signal ratio ranged from 0.12 to 0.30, and the maximum value was smaller than the minimum value in the sublethal TBI groups. Survival was largely prolonged in this group. Four mice died 48 to 63 days after cell inoculation, and presumptive whole-body signals at death were similar to those in the experiments of sublethal TBI ($7.17 \times 10^9$ - $2.15 \times 10^{10}$ photons/s). The other mouse showed a slow increase in whole-body signals and survived much longer (97 days). Despite the marked difference in survival time, the mouse did not differ substantially in presumptive whole-body signals at death from those of other mice ($6.51 \times 10^9$ photons/s).

## Discussion

We investigated the application of in vivo BLI in assessing the effect of TBI in an animal model of a hematological malignancy. First, we evaluated the time course of viable cell numbers and bioluminescence signals after irradiation

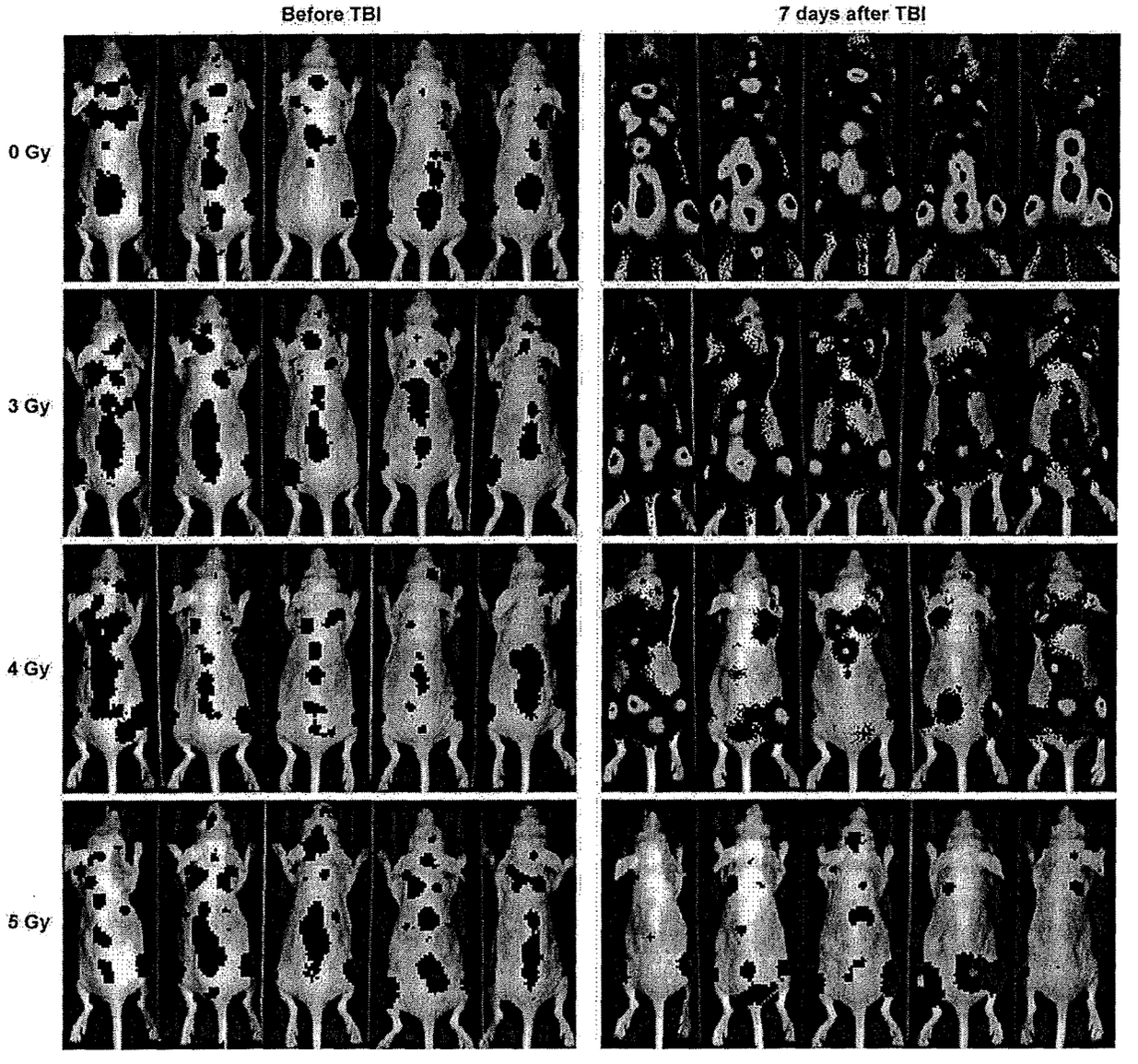


**Figure 2.** Dorsal images of in vivo bioluminescence imaging acquired before and 7 days after sublethal total body irradiation (TBI) (7 and 14 days after cell inoculation). The pseudocolor luminescent image (blue, green, yellow, and red from least to most intense) is overlaid on the grayscale photographic image. The same color scale was used for all panels. Dose-dependent inhibition of disease progression is shown.

of cell suspension to evaluate the validity of bioluminescent signals in tumor monitoring after radiotherapy. Irradiation inhibited cell proliferation transiently, as expected. Luciferase assays demonstrated the inhibitory effect and regrowth similar to viable cell counting, supporting the use of bioluminescence signals as an index of viable tumor burden after irradiation. However, luminescence per cell increased immediately after irradiation, which could cause an overestimation of viable tumor burden in BLI tumor monitoring. It has been reported that ionizing radiation transcriptionally activates the LTRs of Moloney murine sarcoma virus [29], Rous sarcoma virus [30], and human immunodeficiency virus type 1 [31], although it does not influence the activity of the cytomegalovirus immediate-early promoter or the simian virus 40 promoter [30]. In the cells studied in this study, luciferase was expressed under the control of the MMLV LTR, and our observations indicated transcriptional activation of the MMLV LTR by irradiation. Whereas we previously demonstrated that the addition of imatinib to the suspension of Ba/F3-Luc/Wt cells decreases both proliferation index and luminescence per cell [25], increase in luminescence per cell was associated with decrease in proliferation index in the present study. The change in the activity of MMLV LTR cannot be explained by dependence on cell cycle. Ionizing radiation activates various signal transduction pathways [32,33] and many transcription

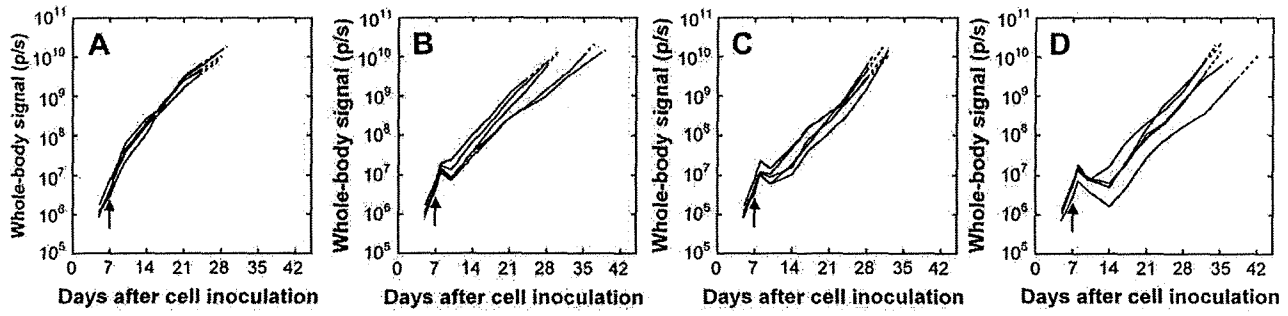


**Figure 3.** Time courses of whole-body bioluminescence signals in each mouse of the control group (**A**) and three sublethal total body irradiation (TBI) groups (**B**, 3 Gy; **C**, 4 Gy; **D**, 5 Gy). TBI was performed 7 days after cell inoculation (arrows). The solid lines were drawn between the measured points, and the broken lines were drawn by extrapolation to the day of spontaneous death.

factors can bind to the enhancer region of MMLV LTR [34,35]. Although the molecular mechanism of the activation of MMLV LTR remains to be elucidated, the results of our cell culture study indicate that luminescence signals from luciferase-expressing cells would approximate viable tumor burden but the relationship may be distorted to some extent early after irradiation.

In mice of a hematological malignancy model, sublethal TBI caused transient inhibition of increase in whole-body signals and prolonged survival in a dose-dependent manner. Although whole-body signals increased on the day after TBI, the increase may not imply increase in tumor burden. Bioluminescence signals immediately after irradiation may have overestimated viable cell numbers due to the activation of the MMLV LTR in vivo as well as in vitro. Whole-body signals 7 days after TBI correlated with survival, indicating the potential of in vivo BLI signals as an early surrogate marker for assessing therapeutic response. In vivo BLI appears to allow early prediction of therapeutic efficacy and may contribute to improving the efficiency of experiments. Moreover, although significant dose dependence was demonstrated for both survival and signal increase during 7 days after TBI, the dependence was more evident for signal increase. Generally, a clearer dose-response relationship can be expected for radiotherapy than for drug therapy due to consistency of delivery and lack of metabolic interference. The rate of tumor regrowth after early response, pretreatment tumor burden, and tumor burden causing death have interindividual variation independent of treatment protocol, which may to some extent obscure the relationship between radiation dose and survival. The clearer dose–response relationship for signal increase suggests that in vivo BLI enables the evaluation of antitumor effects more precisely than survival assessment and that statistically significant results can be obtained more readily in comparing the effects of different treatments. In addition, presumptive whole-body signals at death showed small interindividual differences when compared to the wide signal range observed during the entire course and were independent of radiation dose, supporting the concept that BLI signals reflect disease severity even after treatment.

In mice receiving lethal TBI followed by syngeneic BMT, prolongation of survival and reduction in BLI signals were prominent, suggesting that higher doses can offer better outcomes. Residual signals were demonstrated even at maximal responses, and regrowth was monitored longitudinally. Presumptive whole-body signals at death were similar to those in nonirradiated or sublethally irradiated mice, suggesting that tumor burden causing spontaneous death was not influenced largely by the treatment. Mice that underwent lethal TBI not followed by BMT died while showing weak BLI signals, indicating that death was not due to progression of malignancy but due to the adverse effects of the treatment. Although the dose was known to be lethal and treatment-related death was predictable in the present study, nontumor-related death may occur unexpectedly from treatment-related

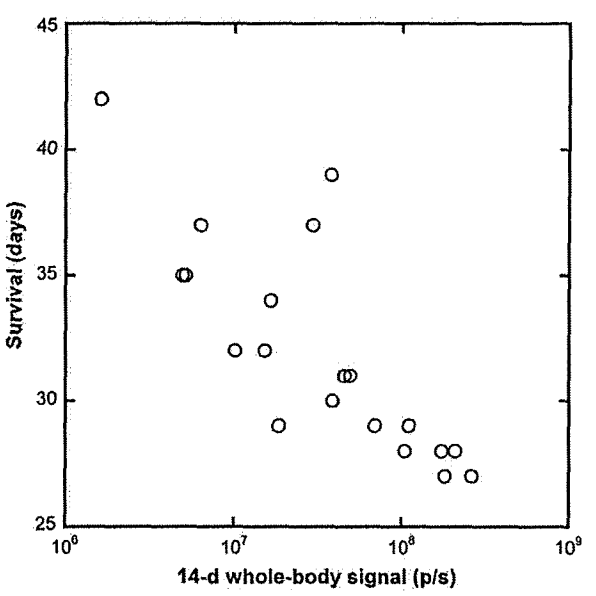


**Figure 4.** Relationship of survival with whole-body signals 14 days after inoculation (7 days after sublethal total body irradiation). A significant negative correlation was demonstrated ($r = -0.8000$, $p < 0.0001$).

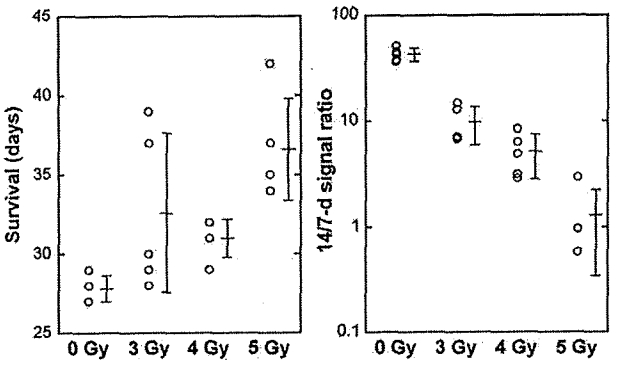


**Figure 5.** Survival (left) and 14/7-day signal ratio (right) in mice receiving various doses of sublethal total body irradiation (TBI). Plots indicate data for individual mice. Mean and standard deviations are also presented. Dose dependence is more evident for the 14/7-day signal ratio, an index of signal increase during 7 days after TBI, than for survival.

damage or incidentally and should be discriminated from death by tumor progression. In vivo BLI allows the evaluation of tumor burden independently of survival and appears to aid the discrimination between tumor-related and nontumor-related deaths and the assessment of antitumor effects in mice that died from nontumor-related causes.

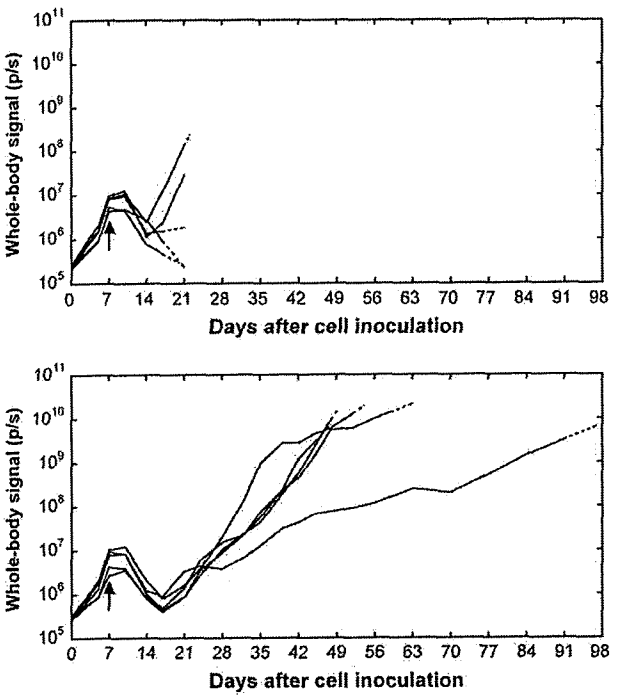


**Figure 6.** Time courses of whole-body bioluminescence signals in each mouse of the total body irradiation (TBI) alone group (upper) and TBI + bone marrow transplantation group (lower). Lethal TBI (7 Gy) was performed 7 days after cell inoculation (arrows). Solid lines were drawn between the measured points, and the broken lines were drawn by extrapolation to the day of spontaneous death. Whole-body signals before cell inoculation, which were not measured in experiments of sublethal TBI, were plotted as day-0 values.

The relationship between in vivo BLI signals and tumor burden may be distorted by various factors. Quantitative estimates of bioluminescence depend on luciferase expression per viable cell, delivery of D-luciferin to luciferase-expressing cells, availability of cofactors (oxygen, adenosine triphosphate, and magnesium) for the luminescent reaction, scattering and absorption of light photons in the tissues, and the determination of ROIs. Our results support bioluminescent evaluation of tumor burden and therapeutic responses in the model used, despite the possible influence of confounding factors. However, substantial signals were not acquired after the first intraperitoneal administration of D-luciferin in nine of 307 BLI studies (2.9%), which appeared to be attributable to bowel injection [9,28] and exemplifies problems with D-luciferin delivery. The possibility of alterations in luciferase activity per viable cell induced by therapeutic intervention was also highlighted, as indicated previously using the MMLV LTR [25] and the cytomegalovirus immediate-early promoter [36,37]. Although the utility of in vivo BLI monitoring of therapeutic efficacy would hold true not only for TBI but also other treatment modalities, it should be noted that luminescence per viable cell may vary early after therapy depending on the type of therapeutic intervention and the promoter driving luciferase expression, resulting in a discrepancy between viable tumor burden and BLI signals. Due to the rapid progression of the disease model used in the present study, only minor differences in survival could be observed. Further evaluation using less aggressive models would be desired.

Our study demonstrates that in vivo BLI allows longitudinal, quantitative evaluation of the response to TBI in a murine hematological malignancy model. Whole-body BLI signals reflect whole-body tumor burden even after TBI with or without BMT, and the antitumor effect can be assessed early, reliably, and independently of survival. Signal change early after treatment, as an alternative to survival, can be used as a marker of therapeutic response for efficient testing of various treatment protocols, and nontumor-related deaths can be determined based on weak BLI signals. Our study also illustrates the need for considering the influence of the treatment on promoter activity, in addition to the general utility of in vivo BLI.

## Acknowledgments

This study was supported in part by Grants-in-Aid for Scientific Research from the Ministry of Education, Culture, Sports, Science and Technology of Japan.

## References

1. Contag CH, Jenkins D, Contag PR, Negrin RS. Use of reporter genes for optical measurements of neoplastic disease in vivo. Neoplasia. 2000;2:41–52.

2. Edinger M, Cao YA, Hornig YS, et al. Advancing animal models of neoplasia through in vivo bioluminescence imaging. Eur J Cancer. 2002;38:2128–2136.
3. Inoue Y, Izawa K, Tojo A, et al. Monitoring of disease progression by bioluminescence imaging and magnetic resonance imaging in an animal model of hematologic malignancy. Exp Hematol. 2007;35: 407–415.
4. Edinger M, Cao YA, Verneris MR, Bachmann MH, Contag CH, Negrin RS. Revealing lymphoma growth and the efficacy of immune cell therapies using in vivo bioluminescence imaging. Blood. 2003; 101:640–648.
5. Shah NP, Tran C, Lee FY, Chen P, Norris D, Sawyers CL. Overriding imatinib resistance with a novel ABL kinase inhibitor. Science. 2004; 305:399–401.
6. Wu KD, Cho YS, Katz J, et al. Investigation of antitumor effects of synthetic epothilone analogs in human myeloma models in vitro and in vivo. Proc Natl Acad Sci U S A. 2005;102:10640–10645.
7. Armstrong SA, Kung AL, Mabon ME, et al. Inhibition of FLT3 in MLL. Validation of a therapeutic target identified by gene expression based classification. Cancer Cell. 2003;3:173–183.
8. Xin X, Abrams TJ, Hollenbach PW, et al. CHIR-258 is efficacious in a newly developed fibroblast growth factor receptor 3-expressing orthotopic multiple myeloma model in mice. Clin Cancer Res. 2006; 12:4908–4915.
9. Paroo Z, Bollinger RA, Braasch DA, et al. Validating bioluminescence imaging as a high-throughput, quantitative modality for assessing tumor burden. Mol Imaging. 2004;3:117–124.
10. Nogawa M, Yuasa T, Kimura S, et al. Monitoring luciferase-labeled cancer cell growth and metastasis in different in vivo models. Cancer Lett. 2005;217:243–253.
11. Szentirmai O, Baker CH, Lin N, et al. Noninvasive bioluminescence imaging of luciferase expressing intracranial U87 xenografts: correlation with magnetic resonance imaging determined tumor volume and longitudinal use in assessing tumor growth and antiangiogenic treatment effect. Neurosurgery. 2006;58:365–372.
12. Smakman N, Martens A, Kranenburg O, Borel Rinkes IH. Validation of bioluminescence imaging of colorectal liver metastases in the mouse. J Surg Res. 2004;122:225–230.
13. Mandl SJ, Mari C, Edinger M, et al. Multi-modality imaging identifies key times for annexin V imaging as an early predictor of therapeutic outcome. Mol Imaging. 2004;3:1–8.
14. Jenkins DE, Oei Y, Hornig YS, et al. Bioluminescent imaging (BLI) to improve and refine traditional murine models of tumor growth and metastasis. Clin Exp Metastasis. 2003;20:733–744.
15. Scatena CD, Hepner MA, Oei YA, et al. Imaging of bioluminescent LNCaP-luc-M6 tumors: a new animal model for the study of metastatic human prostate cancer. Prostate. 2004;15(59):292–303.
16. Zeamari S, Rumping G, Floot B, Lyons S, Stewart FA. In vivo bioluminescence imaging of locally disseminated colon carcinoma in rats. Br J Cancer. 2004;90:1259–1264.
17. Nyati MK, Symon Z, Kievit E, et al. The potential of 5-fluorocytosine/ cytosine deaminase enzyme prodrug gene therapy in an intrahepatic colon cancer model. Gene Ther. 2002;9:844–849.
18. Rehemtulla A, Stegman LD, Cardozo SJ, et al. Rapid and quantitative assessment of cancer treatment response using in vivo bioluminescence imaging. Neoplasia. 2000;2:491–495.
19. Wissink EH, Verbrugge I, Vink SR, et al. TRAIL enhances efficacy of radiotherapy in a p53 mutant, Bcl-2 overexpressing lymphoid malignancy. Radiother Oncol. 2006;80:214–222.
20. Lee CK. Evolving role of radiation therapy for hematologic malignancies. Hematol Oncol Clin North Am. 2006;20:471–503.
21. Kal HB, Loes van Kempen-Harteveld M, Heijenbrok-Kal MH, Struikmans H. Biologically effective dose in total-body irradiation and hematopoietic stem cell transplantation. Strahlenther Onkol. 2006; 182:672–679.
22. Gabriel DA, Shea TC, Serody JS, et al. Cytoprotection by amifostine during autologous stem cell transplantation for advanced refractory hematologic malignancies. Biol Blood Marrow Transplant. 2005;11: 1022–1030.
23. Nieder C, Licht T, Andratschke N, Peschel C, Molls M. Influence of differing radiotherapy strategies on treatment results in diffuse large-cell lymphoma: a review. Cancer Treat Rev. 2003;29:11–19.
24. Gustavsson A, Osterman B, Cavallin-Ståhl E. A systematic overview of radiation therapy effects in non-Hodgkin's lymphoma. Acta Oncol. 2003;42:605–619.
25. Inoue Y, Tojo A, Sekine R, et al. In vitro validation of bioluminescent monitoring of disease progression and therapeutic response in leukaemia model animals. Eur J Nucl Med Mol Imaging. 2006;33:557–565.
26. Copelan EA, McGuire EA. The biology and treatment of acute lymphoblastic leukemia in adults. Blood. 1995;85:1151–1168.
27. Li S, Ilaria RL Jr, Million RP, Daley GQ, Van Etten RA. The P190, P210, and P230 forms of the BCR/ABL oncogene induce a similar chronic myeloid leukemia-like syndrome in mice but have different lymphoid leukemogenic activity. J Exp Med. 1999;189:1399–1412.
28. Baba S, Cho SY, Ye Z, Cheng L, Engles JM, Wahl RL. How reproducible is bioluminescent imaging of tumor cell growth? Single time point versus the dynamic measurement approach. Mol Imaging. 2007;6: 315–322.
29. Lin CS, Goldthwait DA, Samols D. Induction of transcription from the long terminal repeat of Moloney murine sarcoma provirus by UV-irradiation, x-irradiation, and phorbol ester. Proc Natl Acad Sci U S A. 1990;87:36–40.
30. Cheng X, Iliakis G. Effect of ionizing radiation on the expression of chloramphenicol acetyltransferase gene under the control of commonly used constitutive or inducible promoters. Int J Radiat Biol. 1995;67:261–267.
31. Faure E, Cavard C, Zider A, Guillet JP, Resbeut M, Champion S. X irradiation-induced transcription from the HIV type 1 long terminal repeat. AIDS Res Hum Retroviruses. 1995;11:41–43.
32. Dent P, Yacoub A, Contessa J. Stress and radiation-induced activation of multiple intracellular signaling pathways. Radiat Res. 2003;159: 283–300.
33. Chastel C, Jiricny J, Jaussi R. Activation of stress-responsive promoters by ionizing radiation for deployment in targeted gene therapy. DNA Repair. 2004;3:201–215.
34. Kim S, Lee K, Kim MD, et al. Factors affecting the performance of different long terminal repeats in the retroviral vector. Biochem Biophys Res Commun. 2006;343:1017–1022.
35. LoSardo JE, Cupelli LA, Short MK, Berman JW, Lenz J. Differences in activities of murine retroviral long terminal repeats in cytotoxic T lymphocytes and T-lymphoma cells. J Virol. 1989;63:1087–1094.
36. Svensson RU, Barnes JM, Rokhlin OW. Chemotherapeutic agents upregulate the cytomegalovirus promoter: implications for bioluminescence imaging of tumor response to therapy. Cancer Res. 2007;67: 10445–10454.
37. Kim KI, Kang JH, Chung JK, et al. Doxorubicin enhances the expression of transgene under control of the CMV promoter in anaplastic thyroid carcinoma cells. J Nucl Med. 2007;48:1553–1561.